Reconstructing Intra-Annual Growth of Freshwater Mussels Using Oxygen Isotopes

David H. Goodwin[a,*], David P. Gillikin[b], Roxanne Banker[a,1], G. Thomas Watters[c], David L. Dettman[d], Christopher S. Romanek[e]

[a]*Department of Geosciences, Denison University, 100 West College, Granville, OH 43023*
[b]*Department of Geology, Union College, 807 Union Street, Schenectady, NY 12308*
[c]*Department of Evolution, Ecology, and Organismal Biology, The Ohio State University, 1315 Kinnear Road, Columbus, OH 43212*
[d]*Department of Geosciences, The University of Arizona, 1040 East 4th Street, Tucson, AZ 85721*
[e]*Department of Earth and Environmental Sciences, 3300 Poinsett Highway, Greenville, SC 29613*

Abstract

Intra-annual growth rates from the bivalve mollusk *Lampsilis cardium* (Unionidae) were reconstructed using measured oxygen isotope ($\delta^{18}O$) profiles together with high-resolution environmental records. Mussels from a single cohort (2007) were grown in two different settings at the Columbus Zoo & Aquarium Freshwater Mussel Conservation & Research Center (MRC), located in central Ohio, USA. "Outside" specimens were collected from sediment laden cages deployed in the O'Shaughnessy Reservoir. A single "inside" specimen was collected from the raceways in the MRC. Measured $\delta^{18}O_{carb}$ profiles from these specimens were calibrated with a predicted oxygen isotope envelope (i.e., the daily range of potential $\delta^{18}O_{carb}$ values) calculated from hourly water temperatures and weekly $\delta^{18}O_{water}$ samples collected in 2010. This exercise suggests the "outside" specimens commenced 2010 shell deposition in late April and ceased in latest October (six month growing season). In contrast, the "inside" growing season lasted only three months (early July and early September). Calculated daily growth rates from both sites were faster early in the year, but highly episodic throughout. Maximum daily growth rates for the "outside" and "inside" specimens were 300 and 436 μm/day, respectively. Analysis of annual growth rates from the entire cohort suggests the "inside" specimens grew slower following transplantation. In subsequent years, however, their growth rates were nearly identical to the "outside" population. Our results suggest that, despite the fact that both populations have similar annual growth rates, they have different intra-annual growth patterns. Thus, caution should be exercised when extrapolating intra-annaul growth patterns from cultured specimens to natural populations.

Keywords: Bivalve Mollusk, Unionidae, *Lampsilis cardium*, Oxygen Isotope, Growth

1. Introduction

Freshwater mussel (Unionidae) shells contain valuable biogeochemical archives of past environmental conditions, such as: precipitation (Dettman and Lohmann, 2000); temperature (Schöne et al., 2004); and, watershed dynamics (Fry and Allen, 2003; Fritts et al., 2016). Despite their potential as biomonitors, freshwater mussels are among the most endangered organisms in the United States with more than 70% of species being listed as endangered, threatened, or of special concern (Williams et al., 1993). Today, a myriad of factors conspire to threaten the longterm viability of unionoids (Haag, 2012), and North American mussel extinction rates are on a par with those from tropical rainforest communities (Ricciardi and Rasmussen, 1999). Taken together, their precarious future and potential to serve as biomonitors highlight the importance of understanding freshwater mussel ecology in general, and their shell growth in particular.

Unionoid shell growth has been studied for more than 100 years (e.g., Isely, 1913). *Inter-annual* shell growth rates are reconstructed using prominent annual growth increments (Haag, 2009; Black et al., 2010; Haag and Rypel (2011); and see review in Haag, 2012). Reconstructing *intra-annual* growth, however, is less straightforward. In marine bivalves, growth rate estimates are often based on tidal or daily growth increments (e.g., Goodwin et al., 2001; Chauvaud et al., 2005). While putative daily increments have been reported from a few freshwater species (e.g., Dunca and Mutvei, 2001, Schöne et al., 2005), their mechanism(s) of formation are poorly understood and relatively little is known about unionoid intra-annual growth rates.

The few studies that have addressed intra-annual growth in fresheater mussels suggest a relatively wide range of daily growth rates. Dettman et al. (1999) showed that *Lampsilis ovata* and *L. radiata luteola* can add ∼20–30 μm/day. Versteegh et al. (2010) modeled shell growth and

*Corresponding author
Email address: goodwind@denison.edu (David H. Goodwin)
[1]Current Address: Department of Earth and Planetary Sciences, 2119 Earth and Physical Sciences, University of California Davis, One Shields Avenue, Davis, CA 95616

showed that peak rates in *Unio pictorum* were between ~50–100 μm/day. In contrast, Kaandorp et al. (2003) showed that seasonal growth rates in *Anodontites trapesialis* varied between 333 and 500 μm/day, and Kelemen et al. (2017) report growth rates of up to 750 μm/day.

Given the large range of daily growth rates, this study has two primary goals: 1) reconstruct intra-annual growth patterns from *Lampsilis cardium* using high-resolution environmental records; and 2) use daily predicted oxygen isotope ranges (i.e., the *oxygen isotope envelope*) to determine optimal growth temperatures in *L. cardium*. A secondary goal is to compare intra- and inter-annual patterns of growth from animals grown under natural conditions with those grown in captivity.

Growth rate reconstructions commonly take advantage of two distinct methodological approaches. The first uses notching or staining to establish the timing of carbonate precipitation (e.g., Lazareth et al., 2006, 2007; Thébault et al., 2006; Goewert et al., 2007; Ford et al., 2010; Poulain et al., 2010, 2011). However, because freshwater mussels are sensitive to handling stress (Haag and Commens-Carson, 2008), we did not use this approach. Furthermore, since our study site hosts multiple threatened species in interconnected, continuous-flow raceways (see Materials and Methods), *in situ* staining was not an option. The second methodological approach involves aligning *measured* oxygen isotope values from shell carbonate ($\delta^{18}O_{carb}$) with *predicted* $\delta^{18}O_{carb}$ values (Killingley and Berger, 1979; Klein et al., 1996; Kirby et al., 1998; Elliot et al., 2003; Gillikin et al., 2005; Goewert et al., 2007; Goodwin et al., 2009; 2010; Ford et al., 2010; Tynan et al., 2014; Kelemen et al., 2017). This procedure converts isotope samples, which are collected in the *distance* domain, into the *time* domain. Here we employ a modified version of this approach.

Oxygen isotope ratios in bivalve shells are a function of the temperature and isotopic composition of the water ($\delta^{18}O_{water}$) in which they precipitated (Urey, 1948; Urey et al., 1951; Epstein et al., 1951). Therefore, given $\delta^{18}O_{water}$ values and temperature records, one can employ a paleotemperature equation (e.g., Grossman and Ku, 1986) to calculate a predicted $\delta^{18}O_{carb}$ profile. While predicted $\delta^{18}O_{carb}$ profiles show overall patterns of isotopic variation, because they are often calculated using *average* daily temperatures, they do not reflect *diurnal* temperature variation. Goodwin et al. (2001) showed that bivalve mollusks can bias daily shell deposition toward optimal growth temperatures. Accordingly, we calculated the range of $\delta^{18}O_{carb}$ values using daily maximum and minimum temperatures (i.e., the *oxygen isotope envelope*). Measured $\delta^{18}O_{carb}$ values from mussels collected at different times of the year were then calibrated with the oxygen isotope envelope to establish the timing of shell growth.

2. Materials and Methods

The study area is located on the west bank of the O'Shaughnessy Reservoir, a five kilometer, dam-impounded reach of the Scioto River (Figure 1). The Scioto River catchment basin is 16,880 km^2 and empties into the Ohio River at the southern border of the state. The watershed above the O'Shaughnessy Dam drains ~2,500 km^2 of west-central Ohio. The dam spillway elevation is 258.6 m above sea level. The region experiences annual air temperature variability of ~35 °C (1981–2010 average maximum air temperature in July: 29.4 °C; 1981–2010 average minimum air temperature in January: -5.5 °C)(NWS, 2011). Central Ohio receives nearly one meter of precipitation annually. In general, at least five centimeters of precipitation falls each month, with more the 10 cm in May, June, and July (NWS, 2011).

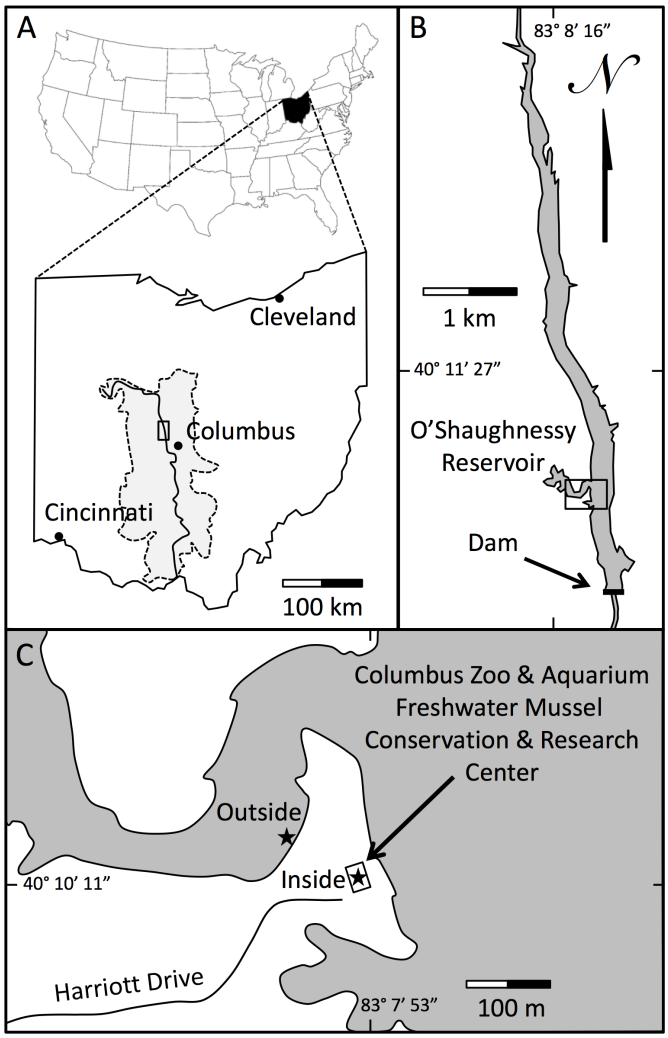

Figure 1: Locality map. (A) Map showing Ohio, major cities, the Scioto River, and its watershed (shaded region). O'Shaughnessy Reservoir is approximately 25 km northwest of Columbus (rectangle). (B) O'Shaughnessy Reservoir on the Scioto River. The study site is on the south-west bank of the reservoir (rectangle). (C) Location of the Freshwater Mussel Research Center. Stars mark the positions of the two study sites.

Specimens used in this study lived at the Columbus Zoo & Aquarium Freshwater Mussel Conservation & Research

Center (MRC; Figure 1). Mussels were collected from two sites at the MRC, one outside and one inside (Figure 1C). All specimens were part of a single original 2007 cohort collected from the Muskingum River near Devola, Ohio. The "outside" site consisted of floating, sediment-laden cages attached to a dock approximately three meters from shore. The "inside" site consists of sediment filled raceways inside the Mussel Research Center supplied with water pumped from the O'Shaughnessy Reservoir. The inlet pipe is located east of the MRC at approximately three meters water depth. Inside water is partially recirculated such that at any given time ∼70% is "old" water and ∼30% is "new" water taken directly from the reservoir.

O'Shaughnessy Reservoir water levels and discharge data were obtained from the USGS National Water Information system (USGS, 2011). Daily precipitation records for 2010 were retrieved for the John Glenn Columbus International Airport weather station (NWS, 2011). The airport is ∼25 km southeast of the Mussel Research Center.

In January 2010, duplicate Onset HOBO® Water Temperature Pro v2 Data Loggers were deployed at each site. Each logger recorded temperature every hour from January 1, 2010; 00:00 AM to December 31, 2010; 23:00 PM (accuracy: 0.2 °C @ 25 °C; resolution: 0.02 °C over 0 °C to 50 °C). Duplicate logger records at each site are highly correlated (correlation coefficients >0.999; n = 8760).

Water samples for stable oxygen and hydrogen isotope ($\delta^{18}O_{water}$ and δD_{water}, respectively) analysis were taken from both sites approximately once a week during 2010 (Outside: n = 46; Inside: n = 49). Aliquots (250 mL) were collected in Nalgene® bottles, capped and sealed with parafilm to prevent evaporation, and refrigerated until analysis. Water samples were analyzed on a Picarro L1102-i Isotopic Liquid Water and Water Vapor Analyzer equipped with a GC-PAL autosampler at the University of Kentucky Stable Isotope Geochemistry Laboratory. Each sample was analyzed twice and average values are reported. International reference standards (VSMOW, SLAP, GISP) were analyzed at the beginning and end of each sequence along with an in-house standard (LEX). In addition, LEX was analyzed after every eighth sample to monitor for analytical drift. The international standards were used for isotopic scale correction using a regression based analysis. The average analytical uncertainty (1σ) for LEX was better than ±0.10‰ for $\delta^{18}O_{water}$ and ±1.0‰ for δD_{water}.

Predicted oxygen isotope values for biogenic carbonate were calculated using observed logger temperatures and $\delta^{18}O_{water}$ values. We used the Dettman et al. (1999) fractionation factor version of Grossman and Ku's (1986) aragonite paleothermometry equation:

$$10^3 \ln\alpha_{\mathrm{carb-water}} = 2.559\ (10^6 \mathrm{T}^{-2}) + 0.715 \qquad (1)$$

where T is temperature in Kelvin, and α_{c-w} is the fractionation factor between carbonate and water. This equation returns $\delta^{18}O_{carb}$ values relative to the VSMOW standard, which we converted to the VPDB scale using $\alpha_{\mathrm{VPDB}}^{\mathrm{VSMOW}} = 1.03091$ (Gonfiantini et al., 1995). We compared predicted $\delta^{18}O_{carb}$ values to observed $\delta^{18}O_{carb}$ data to establish the timing of shell deposition (see Discussion).

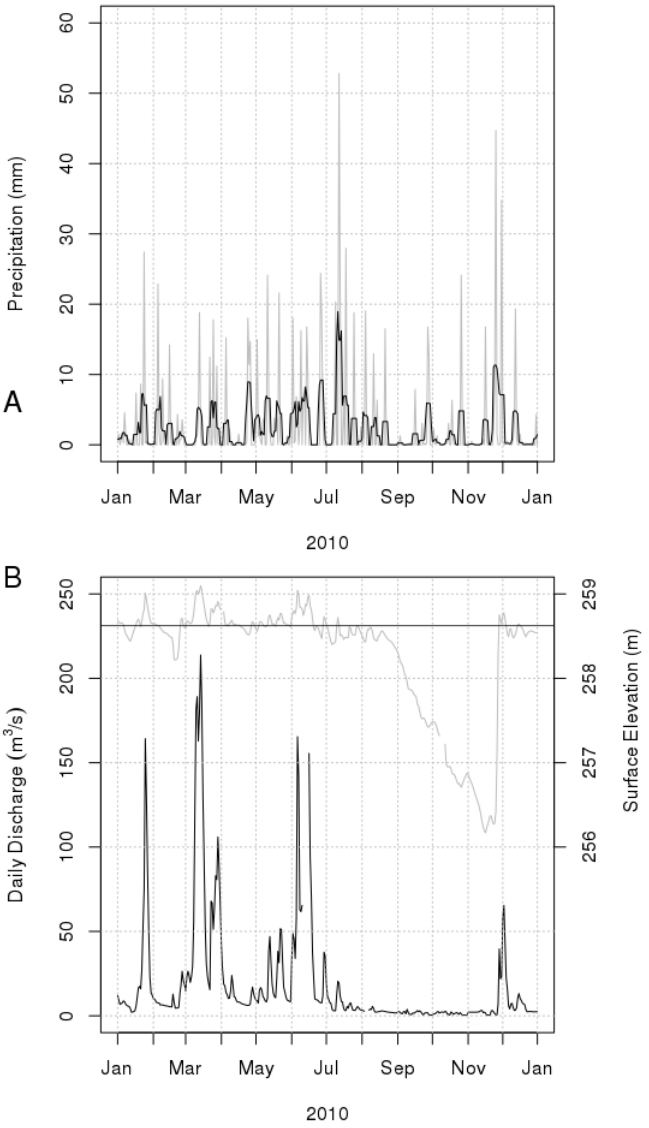

Figure 2: Regional precipitation, reservoir elevation, and discharge data. (A) Daily precipitation (grey line) and 5-day moving average (black line). (B) Daily Scioto River discharge measured at O'Shaughnessy Dam (black line). O'Shaughnessy Reservoir elevation is also shown (grey line). The dam spillway elevation is indicated by the horizontal line at 258.6 m above sea level.

This study focused on *Lampsilis cardium* Rafinesque (1820)—colloquially, the "Plain Pocketbook." The species is relatively large, with valve lengths commonly >15 cm. *L. cardium* is common in Ohio rivers, lakes and ponds. Its overall range extends from the Red River in Canada, through the Great Lakes, to the Mississippi River basin (Watters et al., 2009). Like most freshwater mussels, it is an obligate vertebrate parasite as a larva. *L. cardium* is

Table 1: Collection and sampling information for the *Lampsilis cardium* specimens used in the study.

Specimen No.	Site	Collected	Section Height*	Sample Type	No. of Samples
OR2-A1L	Outside	April 22, 2010	5.73 cm	Micromill	22
OR2-A2R	Outside	April 22, 2010	6.50 cm	Micromill	22
IR3-A1L	Inside	September 22, 2010	3.93 cm	Point Sample	27
OR4-A1L	Outside	September 22, 2010	6.14 cm	Micromill	44
OR6-A1L	Outside†	December 10, 2010	7.15 cm	Micromill	82

*Measured from thick sections; †Transplanted (September 22, 2010 to December 10, 2010)

bradytictic, or a long-term brooder, with spawning taking place in the summer or early autumn, glochidia overwintering in females and subsequently released in the following spring (Watters et al., 2009). Like other members of the genus, *L. cardium* has a modified mantle "lure," which females undulate (Kraemer, 1970) to attract host fish. *L. cardium* shells are aragonitic (Dettman et al., 1999; Goewert et al., 2007).

Living specimens of *L. cardium* were collected on three separate occasions during 2010 (Table 1). Immediately after collection the specimens were sacrificed and the flesh was removed. In the lab, a valve from each specimen was sectioned with a Buehler IsoMet® Low Speed Saw along the dorso-ventral axis of maximum shell height, and ∼1.5 mm thick sections were mounted on glass microscope slides with J-B KwikWeld® epoxy.

Carbonate samples for isotopic analysis were either micromilled or "point sampled" (see below) from thick sections (Table 1). Micromilled samples (50–100 µg) were collected using a computer-controlled X–Y–Z motorized microdrill according to the procedures described by Dettman and Lohmann (1995). These samples, each 50–100 µm wide, ∼150 µm deep, and approximately 3 mm long, were milled parallel to growth lines observed in shell cross-sections. Micromilled samples from OR4-A1L and OR6-A1L were collected dorsoventrally through the most recent prominent growth line to the commissure, and therefore represent the the most recent growth prior to collection (see Haag and Commens-Carson (2008) for a detailed discussion of growth lines in freshwater mussels). No growth lines were observed near the commissure in either OR2-A1L or OR2-A2R. Because the shell of IR3-A1R was so thin, it was point sampled rather than micromilled. Point samples (i.e., drill holes), each with a mass between 50 and 100 µg, were drilled from the outer layer using a 300-micron drill bit. Goodwin et al. (2003) compared the temporal resolution micromilled versus point samples (also see Schöne, 2008). While we expect more time-averaging with point samples, we do not think point sampling significantly effects our results. Point samples were collected through the most recent prominent growth line to the commissure.

Sample distances (Table 2) were measured parallel to shell exteriors. Therefore, distances from the micromilled shells reflect changes in valve height. Distances from the point sampled shell were measured from the centers of successive holes.

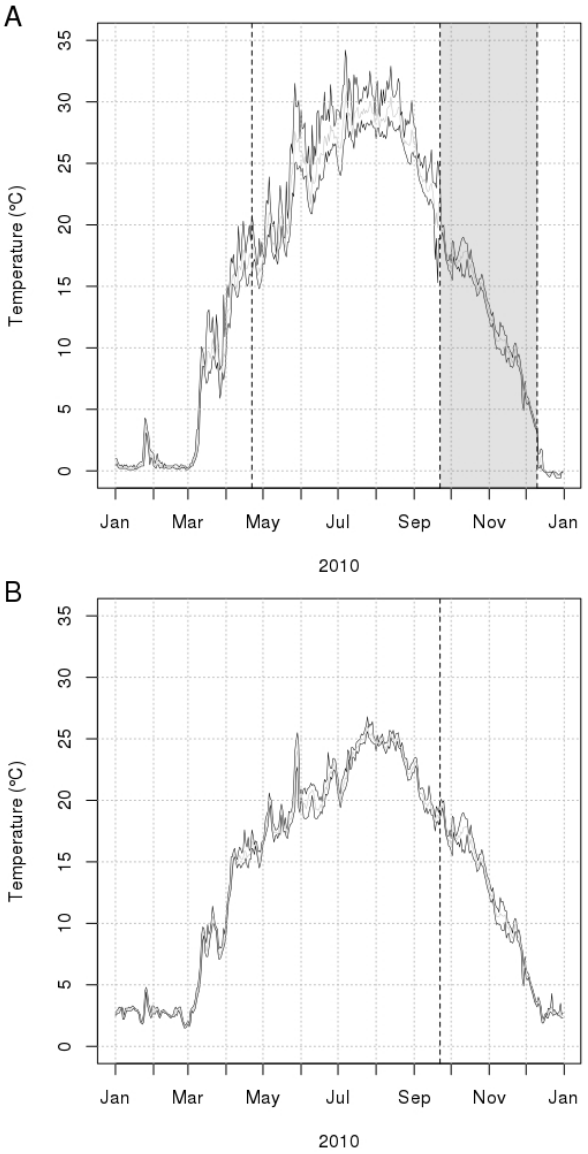

Figure 3: Observed daily maximum, minimum, and average (grey) temperatures. (A) Outside. (B) Inside. Vertical dashed lines indicate specimen collection dates (see Table 1). The shaded box in A represents the transplant interval (Sept. 22 to Dec. 10). Temperatures during this interval are spliced from the inside temperature record.

All carbonate isotopic analyses were performed on a Finnigan MAT 252 mass spectrometer equipped with a

Kiel III automated sampling device at the Environmental Isotope Laboratory, Department of Geosciences, University of Arizona. Samples were reacted with >100% orthophosphoric acid at 70 °C. Results are reported in δ notation (‰) by calibration to the NBS–19 and NBS–18 reference standards (NBS-19: $\delta^{13}C_c = +1.95$ ‰ VPDB and $\delta^{18}O_c = -2.20$ ‰ VPDB; NBS-18: $\delta^{13}C_c = -5.01$ ‰ VPDB and $\delta^{18}O_c = -23.2$ ‰ VPDB). Repeated measurement of standard carbonates resulted in standard deviations (1σ) of ±0.08 and ±0.06‰ for oxygen and carbon, respectively.

Duplicate water samples were collected from both sites approximately every week in 2010 after April 15, 2010 (Outside: n = 35; Inside: n = 38) to determine Chlorophyll *a* concentrations (hereafter, [Chl *a*]). Samples (100–500 ml) were filtered through Whatman® GF/F glass microfiber filters (pore diameter 0.7 μm). Samples were wrapped in aluminum foil and stored frozen. After extraction in 95% acetone, [Chl *a*] was analyzed using standard fluorometric techniques (see Welschmeyer, 1994) with a Turner Designs Trilogy® Laboratory Fluorometer. We report the average [Chl *a*] from duplicate sample pairs in μg/L. The average difference between duplicate samples was 1.18 μg/L.

To compare annual growth rates of the animals grown inside versus outside, valve heights from the entire 2007 cohort (i.e., "outside" and "inside" specimens) were measured seasonally using digital calipers. All living specimens from each site were measured in April and October of 2008 as well as May and October of 2009. A single "inside" specimen could not be located in October of 2008 but was found the following spring.

3. Results

Precipitation (i.e., rainfall amounts), reservoir water level, and discharge data are shown in Figure 2. The region received measurable precipitation on 129 days in 2010, and a total of 91.9 cm for the year (Figure 2A). Approximately 40% of the annual total fell in May, June, and July. In contrast, less than 10% fell between late August and the middle of November. During this relatively dry interval, reservoir elevation fell below the height of the spillway resulting in relatively low river discharge (Figure 2B). As the reservoir continued to fall the sediment laden cages were nearly exposed. Accordingly, on September 22, 2010 the outside specimens were transferred to the inside site. These specimens were subsequently returned to the outside site on December 10, after the reservoir elevation rebounded (Figure 2B). The discharge record shows four episodes of elevated flow: 1) late January, 2) March, 3) early June, and 4) late November–early December.

Observed daily maximum, minimum, and average water temperatures are shown in Figure 3. Because the outside specimens were transplanted inside during the dry autumn months, the temperature data shown in Figure 3A are a spliced record: January 1 to September 22 are outside temperatures, September 23 to December 10 are inside temperatures (shaded region in Figure 3A), and December 11 to December 31 are outside temperatures. The

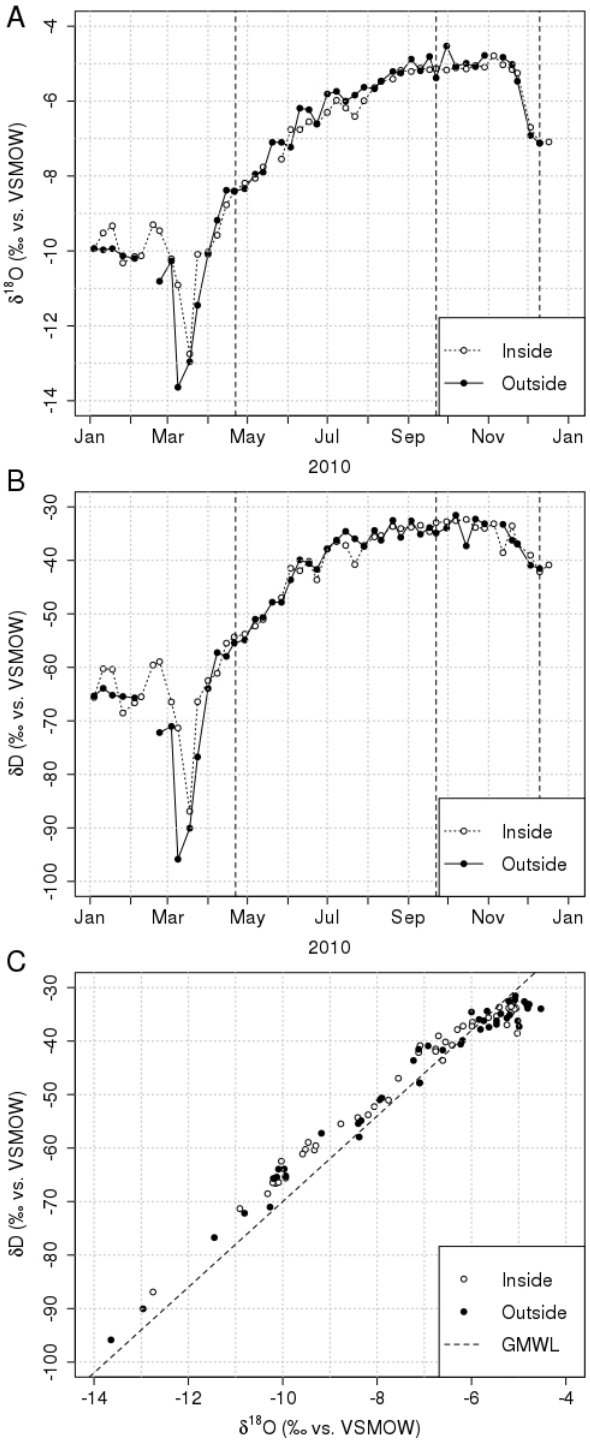

Figure 4: Stable oxygen ($\delta^{18}O_{water}$) and deuterium isotopes (δD_{water}) from weekly samples collected from both sites. (A) $\delta^{18}O_{water}$ values. (B) δD_{water} values. (C) Scatter plot of data from A and B. The Global Meteoric Water Line (dashed line) is shown for comparison. Average analytical uncertainty (1σ) for $\delta^{18}O_{water}$ and δD_{water} were ±0.10‰ and ±1.0‰, respectively. Vertical dashed lines in A and B indicate specimen collection dates (see Table 1).

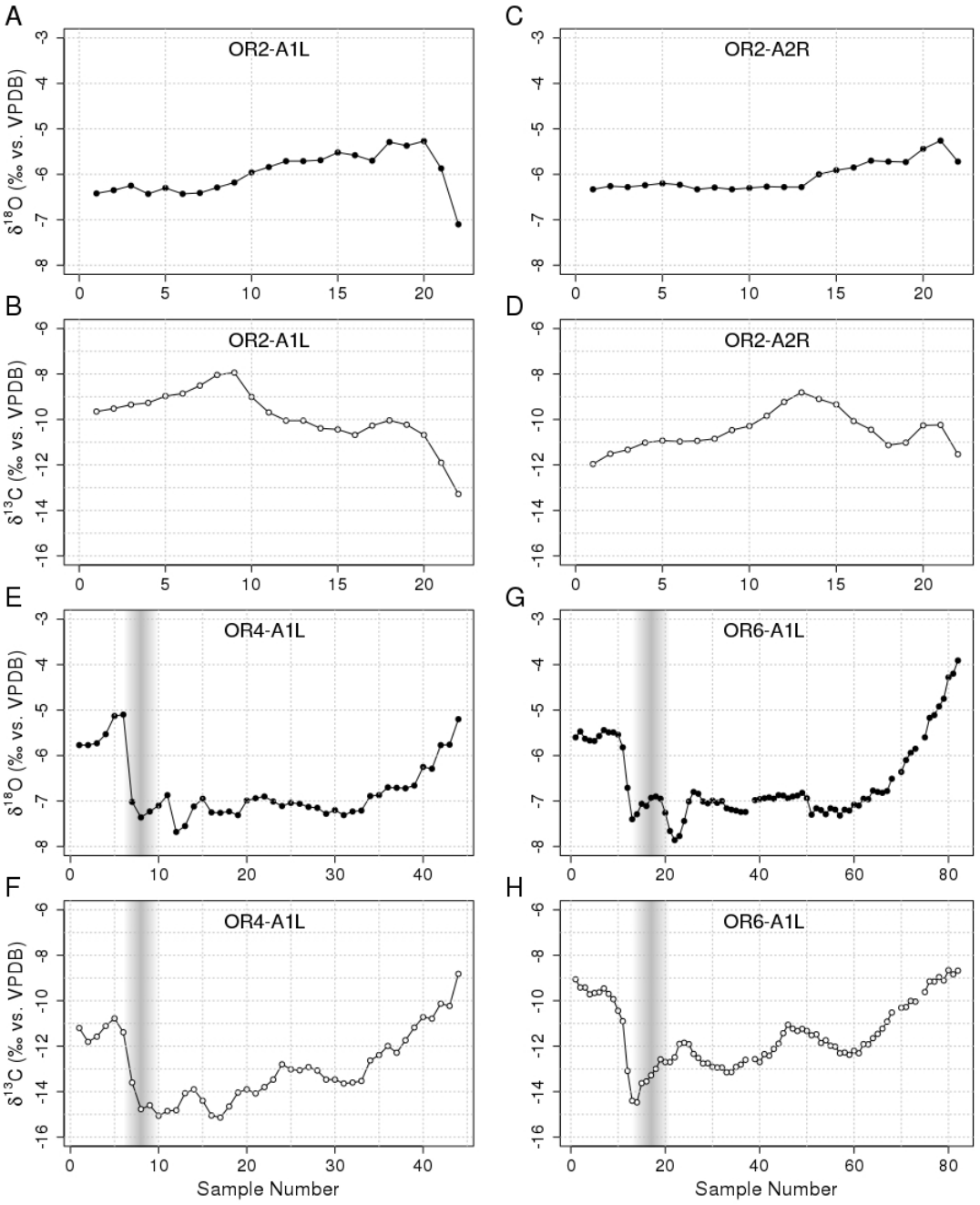

Figure 5: $\delta^{18}O_c$ (filled circles) and $\delta^{13}C_c$ (open circles) profiles from specimens collected outside (see Table 1). (A-B) OR2-A1L; (C-D) OR2-A2R; (E-F) OR4-A1L; (G-H) OR6-A1L. Samples 38, 69, and 74 from OR6-A1L were lost during analysis. The vertical grey lines show the position of growth lines (*sensu* Richardson, 2001) observed in OR4-A1L and OR6-A1L. The average analytical uncertainty (1σ) for $\delta^{13}C_{carb}$ and $\delta^{18}O_{carb}$ were ±0.06 and ±0.08‰, respectively. In all profiles, time passes from left to right and the highest sample number was collected at the commissure (i.e., ventral margin).

maximum temperature recorded was 34.2 °C (July 7) and the minimum temperature, −0.6 °C, was recorded on four consecutive days (December 26–29). The average range of daily water temperature variation was 2.1 °C, although this range increased to more than 3.1 °C between April and September. Temperatures recorded at the inside site (Figure 3B) were not as extreme as those observed outside, likely reflecting the depth of the inlet pipe. Maximum and minimum inside water temperatures were 26.8 °C (July 25) and 1.5 °C (February 26 and 27), respectively. The average daily temperature range was ∼1.0 °C. Unlike the spliced outside record, there was no appreciable change in daily temperature variation.

The four major discharge events (Figure 2B) are correlated with several environmental variables. The first two events are linked with both precipitation (Figure 2A) and

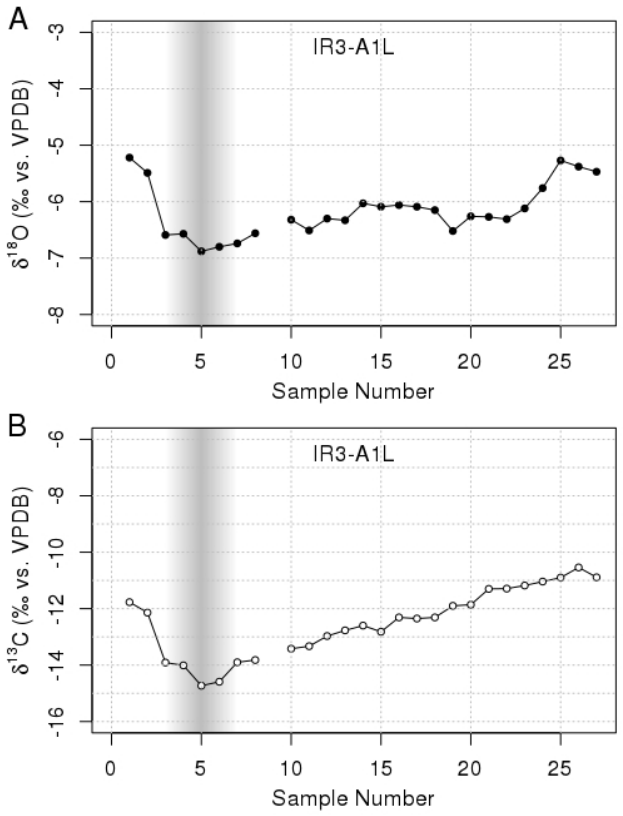

Figure 6: Stable isotope profiles from IR3-A1L. (A) $\delta^{18}O_c$ data. (B) $\delta^{13}C_c$ data. Sample nine was lost during analysis. The average analytical uncertainty (1σ) for $\delta^{13}C_{carb}$ and $\delta^{18}O_{carb}$ were ± 0.06 and ± 0.08‰, respectively. This specimen was collected inside on September 22, 2010. In both profiles, time passes from left to right and the highest sample number was collected at the commissure (i.e., ventral margin).

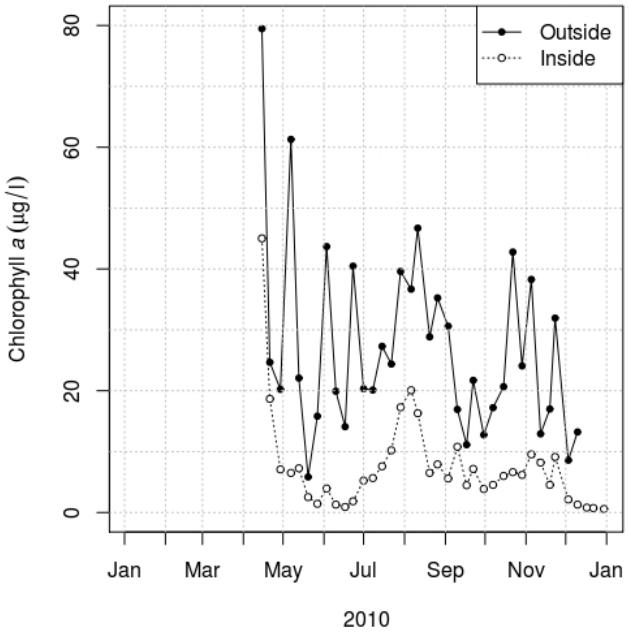

Figure 7: 2010 Chlorophyll *a* concentrations (µg/l) measured outside and inside the Mussel Research Center.

pronounced warming episodes (Figure 3). Thus, these elevated discharge events likely reflects a combination runoff from rain *and* melting of ice and snow in the watershed. The discharge event in early June coincides with an interval of consistent but low intensity precipitation between May 30 and June 17 (see 5-day average in Figure 2A). It is interesting to note that the largest precipitation event of the year (July 12; >5.2 cm) is not associated with elevated discharge. This likely reflects high rates of evapotranspiration and the ability of the soil to store precipitation on the landscape during the summer. The final discharge event is associated with several high-intensity precipitation events that filled the reservoir in late November.

Water oxygen and deuterium isotope data are shown in Figure 4. The $\delta^{18}O_{water}$ profiles from both sites are remarkably similar (Figure 4A). Early in the year, $\delta^{18}O_{water}$ values hover around -10‰, then drop precipitously to approximately -13‰ in March. By early April, $\delta^{18}O_{water}$ values rebounded to their initial values, continued to rise to -5‰ by mid-November, and finally decrease to -7‰ by the end of the year. Although the values differ, the overall pattern of variation of the δD_w data is nearly identical (Figure 4B). The most striking aspect of these data is the pronounced negative excursion in March. This event coincides with a significant warming event (Figure 3A) and the largest discharge event of the year (Figure 2B). The timing of these events suggests the negative excursion reflects the melting and runoff of isotopically light winter precipitation (see Sharp (2006) for a detailed discussion).

Our $\delta^{18}O_{water}$ and δD_{water} data, along with the Global Meteoric Water Line (GMWL; $\delta D_{water} = 8\delta^{18}O_{water} + 10$; Dansgaard, 1964), are shown in Figure 4C. The most negative values (i.e., $\delta^{18}O_{water} < -10.5$‰; $\delta D_{water} < -70$‰) are from the negative isotope excursion in March. These samples, together with those with intermediate values, lie left of the GMWL. This deuterium excess (Dansgaard, 1964) suggests that regional precipitation is influenced by re-evaporated moisture originating west of central Ohio (Gat et al., 1994; Griffis et al., 2016). The most positive values ($\delta^{18}O_{water}$ between -5.5 and -4.5‰; $\delta D_{water} > -40$‰) lie right of the GMWL reflecting evaporative enrichment of the reservoir during the dry period between mid-August and mid-November (see Gat, 1996).

Figures 5 and 6 and Table 2 show the stable isotope values measured from our *L. cardium* shells. In all cases, sample number one represents the ontogenetically youngest material sampled (i.e., toward the umbo), and the highest sample number was collected at the commissure. (Note: While this manuscript will focus on using oxygen isotopes to reconstruct intra-annual growth patterns, the carbon isotope data are presented for completeness. A detailed discussion the $\delta^{13}C_{carb}$ data will be the focus of a forthcoming manuscript.)

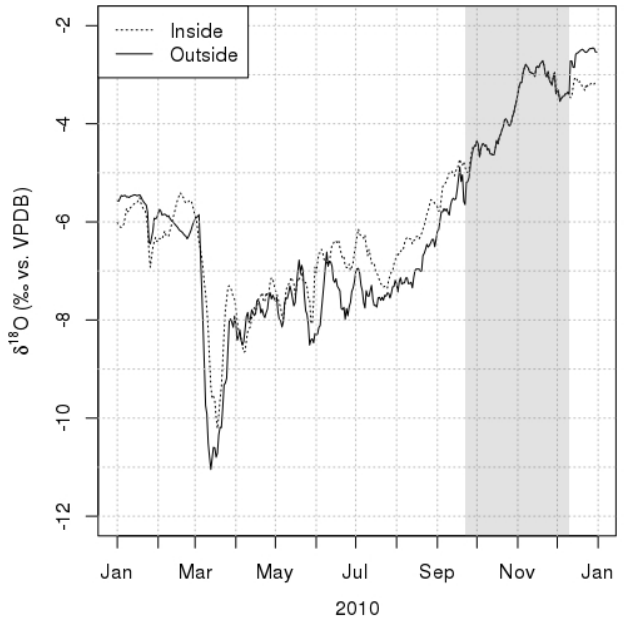

Figure 8: Predicted average daily $\delta^{18}O_{carb}$ values based on average daily temperatures and interpolated $\delta^{18}O_{water}$ values. The shaded region is the transplant interval (Sept. 22 to Dec. 10).

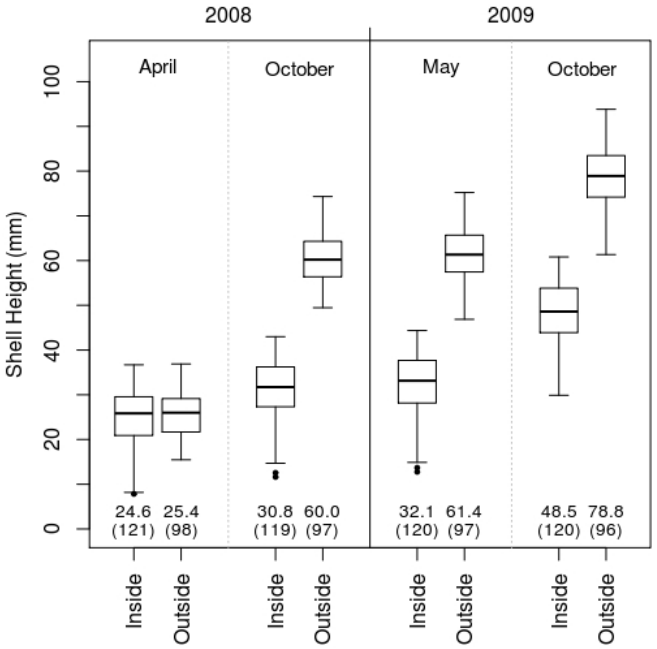

Figure 9: Box plots showing seasonal shell heights of specimens in the original 2007 cohort. Group means (mm) are shown below each box plot. The number of specimens measured during each season is shown in parentheses below the group means.

Twenty-two stable isotope samples were micromilled from both OR2-A1L (Figures 5A–B) and from OR2-A2R (Figures 5C–D). These specimens were collected from the outside site on April 22, 2010. The $\delta^{18}O_{carb}$ values from these profiles increase from ~ -6.5 to ~ -5.5‰, and then fall at the commissure. The final values from OR2-A1L and OR2-A2R are -7.10 and -5.72‰, respectively (Table 2). The overall pattern of $\delta^{13}C_{carb}$ variation in these specimens is similar. Two local maxima are present in each profile (Figures 5B and 5D). Like the $\delta^{18}O_{carb}$ profiles, the final $\delta^{13}C_{carb}$ value from OR2-A1L is more negative than from OR2-A2R (-13.28 versus -11.53‰).

OR4-A1L was collected from the inside site on September 22, 2010. Its stable oxygen isotope data (n=44) are shown in Figure 5E. Initial values range between -6 and -5‰ and then fall to between -8 and -7‰. They remain close to -7‰ in the middle of the profile (samples 15–33), and then rise to -5.20‰ at the commissure (sample 44). The $\delta^{18}O_{carb}$ profile from OR6-A1L (collected on December 10, 2010) is similar (Figure 5G). The most significant difference is that OR6-A1L is approximately 1.3‰ more positive at the commissure (-3.91‰; see Table 2). The $\delta^{13}C_{carb}$ data from OR4-A1L (Figure 5F) and OR6-A1L (Figure 5H) are broadly similar. The most significant difference is that the $\delta^{13}C_{carb}$ values from OR4-A1L are generally more negative than OR6-A1L.

The $\delta^{18}O_{carb}$ and $\delta^{13}C_{carb}$ profiles from IR3-A1L, collected inside the Mussel Research Center on September 22, 2010, are shown in Figure 6. The oxygen isotope values range between -7 and -5‰. The $\delta^{13}C_{carb}$ values range between ~ -15 and -10.5‰.

Conspicuous growth lines (*sensu* Richardson, 2001) were observed in the thick sections from IR3-A1L, OR4-A1L, and OR6-A1L. Their locations are marked with vertical grey bars in Figures 5 and 6. The relative width of the grey bars corresponds to the width of the growth line. Because the margins of these growth lines are somewhat diffuse, they are illustrated with "softened" edges.

Chlorophyll *a* concentrations measured outside and inside the Mussel Research Center are shown in Figure 7. In general, the outside data shows more week-to-week variability than the inside data. [Chl *a*] are consistently higher outside than inside; On average, outside [Chl *a*] are approximately 5 times inside concentrations. The highest concentrations from both sites were recorded in April with a second peak in late July to early August.

Predicted average daily $\delta^{18}O_{carb}$ profiles (Figure 8) were calculated using equation 1, average daily temperatures (Figure 3), and observed $\delta^{18}O_{water}$ values (Figure 4). Because water samples were collected weekly, daily $\delta^{18}O_{water}$ values were linearly interpolated between successive samples. Overall, the predicted $\delta^{18}O_{carb}$ profiles are very similar. Values in January and February range between -6.5 to -5.5‰. In March they drop to between -11 and -10‰ and then rebound to -8‰. They are nearly identical in April and May. During June through September, the outside record is more negative, likely reflecting warmer temperatures outside during the hot summer months. The records are identical in the transplant interval, and then finally diverge in December, reflecting

colder temperatures outside (see Figure 3).

Seasonal measurements of valve heights are shown in Figure 9. In April, 2008, 121 of the originally collected specimens (n = 219) were relocated to the raceways inside the MRC. At the time of transplantation, the mean size of the outside and inside populations was 25.4 and 24.6 mm, respectively. In October, the average height of the outside mussels was 60.0 mm, an increase of 34.6 mm. During the same interval, the inside specimens increased an average of 6.2 mm (μ= 30.8 mm). Over the 2008–2009 winter, the valve height increase in both groups was minimal (outside = 1.4 mm; inside = 1.3 mm). Between May and October of 2009, the outside mussels added 17.4 mm (October mean: 78.8 mm) and the inside mussels added 16.4 mm (October mean: 48.5 mm).

4. Discussion

4.1. The Oxygen Isotope Envelope

Observed oxygen isotopes from shell carbonate are commonly calibrated with predicted values to place microsamples in the time domain (e.g., Killingley and Berger, 1979; Klein et al., 1996; Kirby et al., 1998; Elliot et al., 2003; Gillikin et al., 2005; Goewert et al., 2007; Ford et al., 2010; Goodwin et al., 2010; Tynan et al., 2014). However, while predicted $\delta^{18}O_{carb}$ values accurately show overall patterns of isotopic variation (Figure 8), they are often calculated using *average* daily temperatures, thus they do not reflect *diurnal* temperature variation.

Goodwin et al. (2001) showed that bivalve mollusks can bias daily shell deposition toward optimal growth temperatures. That is, in cooler months they preferentially grew during the warm hours of the day when temperatures approached optimal growth conditions. Conversely, clams grew faster during the cool part of the day in the hottest summer months. These observations suggest matching observed data with *average* daily predicted $\delta^{18}O_{carb}$ values may lead to erroneous date assignments. For example, carbonate deposited in the spring may be falsely assigned a date with warmer average daily temperatures. Similarly, summer growth could be associated with dates with cooler average daily temperatures either earlier *or* later in the year.

That bivalve mollusks shell deposition may be weighted toward optimal growth temperatures highlights the need to consider diurnal temperature variation when matching predicted and observed $\delta^{18}O_{carb}$ values. Accordingly, here we use daily maximum and minimum temperatures (Figure 3) to calculate the *range* of potential $\delta^{18}O_{carb}$ values for each day. In a perfect world we would also use daily maximum and minimum water oxygen isotope values to calculate the predicted range of $\delta^{18}O_{carb}$ values. However, since collecting hourly water samples for a complete year was impractical, we assumed minimal daily variation and used observed $\delta^{18}O_{water}$ values from weekly water samples (Figure 4). As with the predicted average daily $\delta^{18}O_{carb}$ profiles (Figure 8), we linearly interpolated $\delta^{18}O_{water}$ values for days that were not sampled (see Section 3).

Figures 10 and 11 show the predicted $\delta^{18}O_{carb}$ values for the outside and inside sites, respectively. Because of the inverse relationship between temperature and the oxygen isotope ratio of carbonate, the upper line corresponds with daily minimum temperatures and the lower line with daily maxima. The region between the two curves represents all of the potential oxygen isotope values for shell carbonate deposited during 2010—in other words, the *oxygen isotope envelope*. Because bivalve mollusks in general (e.g., Chauvaud et al., 2005; Wanamaker et al., 2007), and *L. cardium* in particular (Dettman et al. 1999; Goewert et al., 2007), precipitate their shells in isotopic equilibrium with the water in which they grow, measured $\delta^{18}O_{carb}$ values should lie within the oxygen isotope envelope.

4.2. Matching Predicted and Observed $\delta^{18}O_{carb}$ Values

Numerous studies have shown that rates of shell growth in freshwater mussels vary throughout the year (Howard 1921; Chamberlain 1931; Negus 1966; Kesler et al. 2007, Rypel et al. 2008, Versteegh et al. 2009; Dycus et al. 2015; Kelemen et al. 2017). Furthermore, in many species, shell deposition halts altogether below specific temperature thresholds (e.g., Negus 1966; Schöne et al. 2004; Versteegh et al. 2010). Working with *L. cardium*, Dettman et al. (1999) and Goewert et al. (2007) independently demonstrated that shell deposition ceases below ∼12 °C. While growth-limiting temperatures can change through ontogeny (Goodwin et al., 2003; Schöne et al. 2003), the specimens used by both Dettman et al. (1999) and Goewert et al. (2007) were similar sizes and ages to those used here, thus we initially assume no growth occurred below at least 12 °C. Observed average daily temperatures remained above this threshold between April 2, 2010 and November 4, 2010 (Figure 3), suggesting that the growing season should extend from early spring and through mid-autumn.

4.2.1. Outside Specimens: Pre-2010 Shell Growth

OR2-A1L and OR2-A2R were collected on April 22, 2010 (Table 1). The maximum *predicted* $\delta^{18}O_{carb}$ value on that day was −7.51‰ (see Figure 10). The $\delta^{18}O_{carb}$ value of the last sample from OR2-A2R, however, is nearly two permil more positive (−5.72‰; Table 2). This observations suggests OR2-A2R had not begun depositing shell material during the 2010 growing season prior to collection. While there are similar predicted $\delta^{18}O_{carb}$ values *earlier* in 2010 (see Figures 8 and 10), they reflect water temperatures less than 5 °C—well below the 12 °C threshold for growth. The $\delta^{18}O_{carb}$ profile from OR2-A1L is very similar to the profile from OR2-A2R with the notable exception that the final value is ∼1.4‰ more negative (−7.10‰; Table 2). While this is closer to predicted values on April, 22, it still lies well outside (0.41‰) the oxygen isotope envelope. That said, this sample is more than 1‰ more negative than the 12 preceding samples (Figure 5A;

Table 2: Stable oxygen and carbon isotope data from shells used in this study. Specimen–Sample: specimen and isotope sample number; $\delta^{18}O_{carb}$ and $\delta^{13}C_{carb}$: oxygen and carbon isotope values, respectively; Date: calendar date assigned to each sample; Distance: cumulative sample distance in mm, beginning with the first 2010 sample.

Specimen–Sample	$\delta^{18}O_{carb}$ (‰ vs. VPDB)	$\delta^{13}C_{carb}$ (‰ vs. VPDB)	Date	Distance (mm)
OR2-A1L–1	−6.42	−9.65	—	—
2	−6.35	−9.52	—	—
3	−6.25	−9.35	—	—
4	−6.43	−9.27	—	—
5	−6.30	−8.97	—	—
6	−6.43	−8.86	—	—
7	−6.41	−8.51	—	—
8	−6.29	−8.04	—	—
9	−6.18	−7.94	—	—
10	−5.96	−9.01	—	—
11	−5.84	−9.69	—	—
12	−5.71	−10.05	—	—
13	−5.71	−10.05	—	—
14	−5.69	−10.39	—	—
15	−5.52	−10.44	—	—
16	−5.58	−10.68	—	—
17	−5.70	−10.27	—	—
18	−5.29	−10.04	—	—
19	−5.37	−10.23	—	—
20	−5.27	−10.68	—	—
21	−5.87	−11.90	—	—
22	−7.10	−13.28	—	—
OR2-A2R–1	−6.33	−11.96	—	—
2	−6.26	−11.51	—	—
3	−6.28	−11.33	—	—
4	−6.24	−11.02	—	—
5	−6.20	−10.93	—	—
6	−6.23	−10.97	—	—
7	−6.33	−10.94	—	—
8	−6.29	−10.85	—	—
9	−6.33	−10.47	—	—
10	−6.30	−10.29	—	—
11	−6.27	−9.84	—	—
12	−6.28	−9.23	—	—
13	−6.28	−8.81	—	—
14	−6.00	−9.10	—	—
15	−5.91	−9.34	—	—
16	−5.85	−10.07	—	—
17	−5.70	−10.45	—	—
18	−5.72	−11.13	—	—
19	−5.73	−11.02	—	—
20	−5.44	−10.26	—	—
21	−5.26	−10.24	—	—
22	−5.72	−11.53	—	—
IR3-A1L–1	−5.22	−11.77	—	—
2	−5.49	−12.14	—	—
3	−6.59	−13.91	06/04	0.434
4	−6.57	−14.01	06/06	0.822
5	−6.88	−14.73	06/08	1.167
6	−6.80	−14.59	06/10	1.597
7	−6.74	−13.90	06/12	1.999
8	−6.56	−13.82	06/14	2.290
9	—	—	06/16	2.733
10	−6.32	−13.42	06/18	3.142
11	−6.51	−13.33	07/01	3.541
12	−6.30	−12.97	07/02	3.962
13	−6.33	−12.77	07/03	4.369
14	−6.03	−12.60	07/04	4.779
15	−6.09	−12.82	07/05	5.174
16	−6.06	−12.31	07/06	5.610
17	−6.09	−12.35	07/07	6.019
18	−6.15	−12.31	07/08	6.416
19	−6.52	−11.90	07/09	6.838
20	−6.52	−11.86	08/09	7.215
21	−6.27	−11.30	08/13	7.631
22	−6.31	−11.29	08/17	8.080
23	−6.12	−11.18	08/21	8.527
24	−5.76	−11.04	08/24	8.900
25	−5.27	−10.90	08/27	9.338
26	−5.38	−10.54	08/29	9.709
27	−5.47	−10.89	09/04	10.169
OR4-A1L–1	−5.77	-11.20	—	—
2	−5.77	-11.81	—	—
3	−5.73	−11.58	—	—
4	−5.53	−11.11	—	—
5	−5.13	−10.78	—	—
6	−5.10	−11.39	—	—
7	−7.02	−13.60	—	—
8	−7.36	−14.77	04/27	0.229
9	−7.23	−14.60	05/13	0.457
10	−7.10	−15.06	05/18	0.686
11	−6.87	−14.85	05/21	0.914
12	−7.68	−14.82	05/24	1.264
13	−7.55	−14.07	06/06	1.614
14	−7.12	−13.90	06/08	1.964
15	−6.95	−14.40	06/10	2.314
16	−7.25	−15.05	06/12	2.664
17	−7.26	−15.14	06/14	3.014
18	−7.23	−14.65	06/16	3.314
19	−7.31	−14.04	06/18	3.614
20	−6.99	−13.90	06/30	3.914
21	−6.94	−14.08	07/01	4.214
22	−6.90	−13.80	07/02	4.514
23	−7.01	−13.47	07/03	4.814
24	−7.11	−12.80	07/04	5.114
25	−7.04	−13.02	07/05	5.334
26	−7.06	−13.06	07/06	5.554
27	−7.13	−12.92	07/07	5.774
28	−7.15	−13.07	07/12	5.994
OR4-A1L–29	−7.28	−13.47	07/17	6.214
30	−7.20	−13.47	07/21	6.434
31	−7.31	−13.64	07/26	6.654
32	−7.23	−13.60	07/30	6.874
33	−7.21	−13.53	08/04	7.100
34	−6.89	−12.63	08/08	7.325
35	−6.87	−12.39	08/13	7.550
36	−6.70	−11.99	08/17	7.764
37	−6.71	−12.29	08/22	7.978
38	−6.72	−11.74	08/26	8.192
39	−6.66	−11.18	08/31	8.406
40	−6.25	−10.72	09/04	8.620
41	−6.29	−10.79	09/09	8.816
42	−5.77	−10.13	09/13	9.012
43	−5.76	−10.23	09/18	9.208
44	−5.20	−8.82	09/22	9.403
OR6-A1L–1	−5.60	−9.06	—	—
2	−5.47	−9.42	—	—
3	−5.63	−9.42	—	—
4	−5.67	−9.72	—	—
5	−5.68	−9.66	—	—
6	−5.57	−9.63	—	—
7	−5.44	−9.46	—	—
8	−5.49	−9.70	—	—
9	−5.49	−9.93	—	—
10	−5.54	−10.44	—	—
11	−5.82	−10.90	—	—
12	−6.71	−13.09	—	—
13	−7.40	−14.40	04/27	0.151
14	−7.29	−14.47	05/10	0.302
15	−7.06	−13.63	05/18	0.453
16	−7.11	−13.55	05/19	0.604
17	−6.93	−13.28	05/20	0.755
18	−6.90	−13.00	05/21	0.905
19	−6.95	−12.58	05/22	10.56
20	−7.26	−12.70	05/23	1.207
21	−7.66	−12.70	05/24	1.358
22	−7.86	−12.49	05/25	1.509
23	−7.77	−11.90	06/05	1.766
24	−7.44	−11.85	06/06	2.023
25	−7.01	−11.91	06/07	2.280
26	−6.80	−12.34	06/08	2.537
27	−6.84	−12.52	06/09	2.794
28	−7.01	−12.76	06/10	3.051
29	−7.05	−12.75	06/11	3.308
30	−6.99	−12.91	06/12	3.565
31	−7.04	−12.94	06/13	3.822
32	−7.00	−12.94	06/14	4.079
33	−7.16	−13.15	06/15	4.354
34	−7.19	−13.14	06/16	4.429
35	−7.21	−12.91	06/17	4.604
36	−7.24	−12.81	06/18	4.779
37	−7.24	−12.60	06/19	4.954
38	—	—	06/20	5.129
39	−6.98	−12.57	06/27	5.304
40	−6.96	−12.70	06/28	5.479
41	−6.94	−12.35	06/29	5.654
42	−6.92	−12.42	06/30	5.829
43	−6.95	−12.12	07/01	6.004
44	−6.87	−11.89	07/02	6.179
45	−6.88	−11.43	07/03	6.334
46	−6.94	−11.06	07/04	6.489
47	−6.90	−11.23	07/05	6.639
48	−6.88	−11.33	07/06	6.789
49	−6.82	−11.24	07/07	6.939
50	−6.94	−11.33	07/08	7.089
51	−7.30	−11.52	07/09	7.239
52	−7.16	−11.48	07/12	7.389
53	−7.20	−11.86	07/15	7.539
54	−7.29	−11.74	07/18	7.748
55	−7.16	−11.98	07/21	7.957
56	−7.19	−12.02	07/24	8.165
57	−7.32	−12.31	07/27	8.374
58	−7.19	−12.28	07/30	8.583
59	−7.21	−12.38	08/02	8.792
60	−7.08	−12.20	08/05	9.000
61	−7.10	−12.31	08/08	9.209
62	−6.95	−11.91	08/11	9.369
63	−6.96	−11.92	08/14	9.529
64	−6.77	−11.95	08/17	9.689
65	−6.80	−11.46	08/20	9.849
66	−6.82	−11.23	08/23	10.009
67	−6.78	−10.92	08/26	10.169
68	−6.51	−10.52	08/29	10.329
69	—	—	09/01	10.489
70	−6.36	−10.31	09/04	10.649
71	−6.10	−10.28	09/07	10.809
72	−5.94	−10.01	09/10	10.973
73	−5.85	−10.04	09/13	11.136
74	—	—	09/16	11.300
75	−5.60	−9.62	09/19	11.464
76	−5.17	−9.15	09/22	11.627
77	−5.11	−9.16	09/28	11.791
78	−4.92	−8.96	10/04	11.955
79	−4.75	−9.11	10/10	12.118
80	−4.28	−8.66	10/16	12.282
81	−4.20	−8.84	10/22	12.445
82	−3.91	−8.68	10/28	12.609

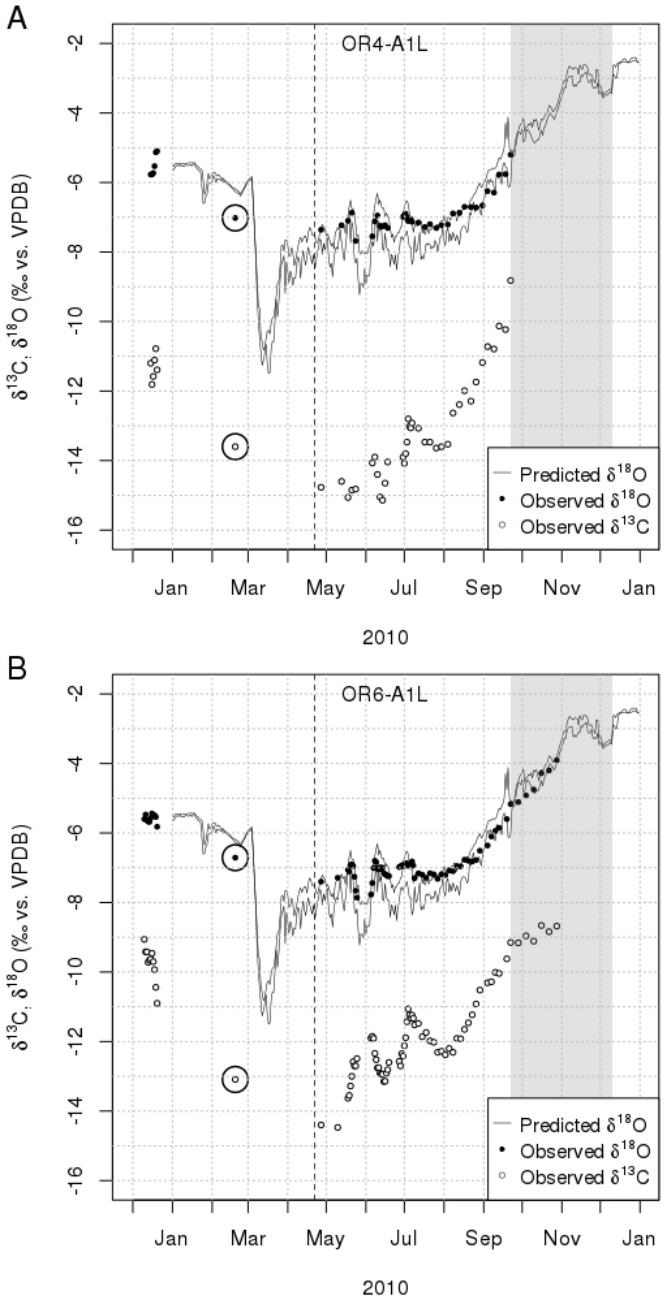

Figure 10: Predicted outside daily maximum and minimum $\delta^{18}O_{carb}$ values for 2010. Observed $\delta^{18}O_{carb}$ (filled circles) and $\delta^{13}C_{carb}$ (open circles) are fit to the predicted oxygen isotope envelope. (A) OR4-A1L. (B) OR6-A1L. The vertical dashed lines mark April 22, the date the OR2 specimens were collected. 2009 samples were arbitrarily placed in December of 2009. The circled values are from samples that contained material deposited in 2009 *and* 2010. These samples are not assigned a date, rather they placed at the midpoint between the 2009 samples and the earliest 2010 sample to highlight their time-averaging. 1σ errors for both water and carbonate samples are smaller than the solid black circles. The shaded region is the transplant interval.

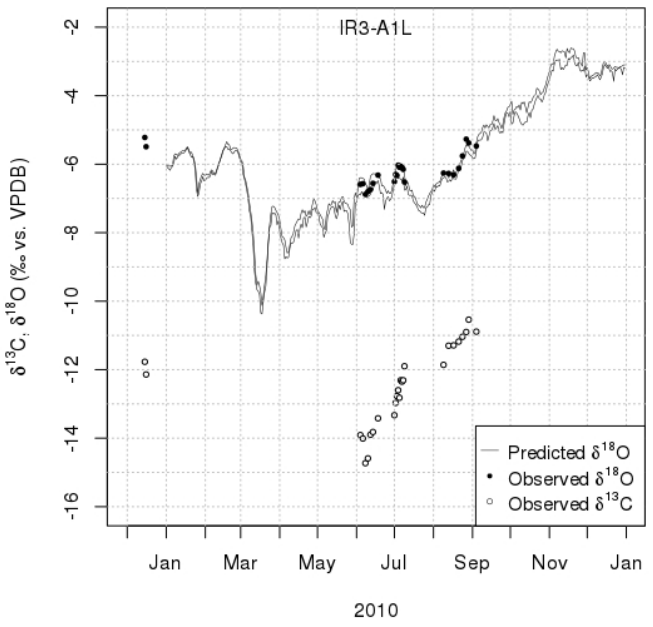

Figure 11: Predicted inside daily maximum and minimum values for 2010. Observed $\delta^{18}O_{carb}$ (filled circles) and $\delta^{13}C_{carb}$ (open circles) are fit to the predicted envelope. 1σ errors for both water and carbonate samples are smaller than the solid black circles. 2009 samples were arbitrarily placed in December of 2009.

Table 2), suggesting this sample may contain some carbonate deposited at the beginning of the 2010 growing season. In other words, that −7.10‰ is lower than 2009 samples and higher than predicted values for the spring of 2010 may reflect a time-averaging sample containing carbonate precipitated in late 2009 and early 2010. Similar time-averaging is also apparent in the profiles from mussels collected later in the year (see below). Taken together, the data from OR2-A1L and OR2-A2R suggest the 2010 growing season began in mid- to late April.

The $\delta^{18}O_{carb}$ variation from the latter half of the OR2 profiles (Figures 5A and 5C) is mirrored by the *initial* $\delta^{18}O_{carb}$ variation from OR4-A1L and OR6-A1L (Figures 5E: samples 1–6; and 5G: samples 1–11). In all four profiles, these $\delta^{18}O_{carb}$ values hover between −6 and −5‰, show similar trends, and precede a ∼2‰ drop in $\delta^{18}O_{carb}$ values (except in OR2-A2R). Likewise, their $\delta^{13}C_{carb}$ profiles closely resemble each other (see Figure 5). This similitude suggests all four mussels deposited this shell material at the same time—likely late in 2009. This conclusion is supported by the presence of prominent growth lines in OR4-A1L and OR6-A1L immediately following the putative 2009 samples (Figures 5E and 5G). As no growth lines were observed in the OR2 shells, they must reflect shell deposition early in the 2010 growing season but after April 22. Accordingly, because the first six samples from OR4-A1L were milled from shell material deposited before the growth line they likely represent shell deposited in 2009 (see Figure 10A). By the same reasoning, the first 11 samples from OR6-A1L are from 2009 (Figure 10B).

The next sample in each profile (OR4-A1L: sample 7, −7.02‰; OR6-A1L: sample 12, −6.71‰; Table 2) is asso-

ciated with the pronounced ∼2‰ drop in $\delta^{18}O_{carb}$ values. In OR4-A1L, this sample partially overlaps growth band (Figure 5E), while in OR6-A1L, it was drilled from shell that predates the growth line (Figure 5G). In each case, these $\delta^{18}O_{carb}$ values do not fall within the oxygen isotope envelope until mid to late-May (see Figure 10). Subsequent samples, however, collected from within the growth line, lie within the predicted range as early as late April (Figure 10). This suggests that sample 7 and sample 12 were collected from shell deposited before late April. Furthermore, because these samples have $\delta^{18}O_{carb}$ values between the 2009 samples and the earliest 2010 samples, they are likely time-averaged, with some of the sample taken from shell deposited in late 2009 and some in early 2010. Accordingly, they cannot reasonably be assigned dates in 2010. These samples are circled in Figure 10. Their position does not imply shell growth in February, rather they were simply placed between the 2009 samples and the earliest 2010 sample to highlight their time-averaging.

4.2.2. Outside Specimens: 2010 Shell Growth

The remainder of the samples from OR4-A1L (8–44) and OR6-A1L (13–82) were collected from shell deposited in 2010, and can confidently be fit in the oxygen isotope envelope. These samples were assigned dates within the oxygen isotope envelope using the following procedure: 1) The value of the first observed $\delta^{18}O_{carb}$ sample from 2010 was compared with the predicted envelope after April 22. Once the sample value fit inside the envelope, it was assigned a date. 2) Subsequent samples that defined discernible, sub-annual patterns (e.g., concave-down cycles, etc.), were compared with the oxygen isotope envelope to identify similar "local" patterns of variability. Once these local patterns were matched, dates were assigned to individual samples. 3) The final sample from OR4-A1L (−5.20‰) was fit to oxygen isotope envelope on the last possible day prior to collection (i.e., September 22). Because sample number 76 from OR6-A1L had a nearly identical value (−5.17‰) it was assigned the same date. 4) The final sample form OR6-A1L was assigned the last possible date when the sample value fit inside the predicted envelope. 5) Finally, all intervening samples were assigned dates using linear interpolation between previously dated samples. There is a one-to-one correspondence between samples and dates (i.e., each sample was assigned a unique date, and no dates were associated with multiple samples). Finally, because we chose not to stain or mark our specimens during the growing season, it is possible that some of our date assignments are incorrect. That said, our conservative fitting approach likely results in dating errors of less than one week.

The first unequivocal 2010 sample from each mussel have nearly identical $\delta^{18}O_{carb}$ values (OR4-A1L: sample 8, −7.36‰; OR6-A1L: sample 13, −7.40‰; Table 2). The first day after April 22 with a predicted maximum $\delta^{18}O_{carb}$ value greater than −7.36‰ was April 27. The maximum value on the preceding day was −7.44‰. These values bracket the first 2010 samples, suggesting both specimens began growing on April 27, 2010 (Figure 10).

The next samples in each $\delta^{18}O_{carb}$ profile from two distinct concave-down cycles (see Figures 5E and 5G; OR4-A1L: samples 9–12 and 13–19; OR6-A1L: samples 14–22 and 23–37). The first cycle fits the oxygen isotope envelope in mid-May, and the second fits the envelope in early to mid-June (Figure 10). These date assignments suggest that little to no growth occurred during the three pronounced warming events that occurred in early May, late May to early June, and late June (see Figure 3A).

Eight samples from OR4-A1L (20–27) were assigned to consecutive days beginning June 30 (Figure 10A; Table 2), suggesting shell deposition resumed in latest June. All of these samples have values of approximately −7‰. Similarly, 12 consecutive samples from OR6-A1L (39–50) have $\delta^{18}O_{carb}$ values of ∼ −7‰ (Table 2), and were assigned dates between June 27 and July 8 (Figure 10B; Table 2). In each shell, these samples coincide with a positive peak in the oxygen isotope envelope (Figure 10). This peak is the only time between mid-June and the end of July when envelope encompasses values of −7‰, suggesting these date assignments are reasonable.

Growth rates during this interval are relatively fast. The predicted values in this peak are greater than −7‰ for six days (Figure 10: June 30 to July 5). In contrast, eight samples from OR4-A1L and 12 from OR6-A1L had values of approximately −7‰. Despite the fact that these samples were assigned dates with longer durations (i.e., 8 and 12 days), they were all likely deposited during this six-day interval. This suggests each sample represents less than a single day of growth. In fact, assuming continuous and uniform growth, the OR4-A1L samples represent 18 hours of growth (144 hours/8 samples) and the OR6-A1L samples represent 12 hours of growth (144 hours/12 samples). Of course, if shell deposition was not continuous, sample temporal resolution was even higher. This observation is particularly significant because, like marine bivalves, which can have micromilled sample resolutions of as little as four hours (D. Dettman, unpublished data), freshwater mussel shells contain a very high-resolution record of continental environmental conditions (also see Dettman et al., 1999; Kaandorp et al., 2003; Kelemen et al., 2017).

The remaining samples from OR4-A1L (28–44) define a generally increasing trend (Figure 5E). The $\delta^{18}O_{carb}$ value of the first sample in this series (−7.15‰; Table 2) is to similar the preceding samples, which were assigned dates in early July. The $\delta^{18}O_{carb}$ value of the last sample is −5.20‰. Because this value lies within the predicted oxygen isotope envelope on September 22 (i.e., date of collection), OR4-A1R was likely growing when it was collected. To establish the timing of deposition of the intermediate samples we assumed constant growth and assigned dates in 4-5 day increments (see Figure 10A).

A similar approach was used to date the remaining OR6-A1L samples (51-82). The first sample in this se-

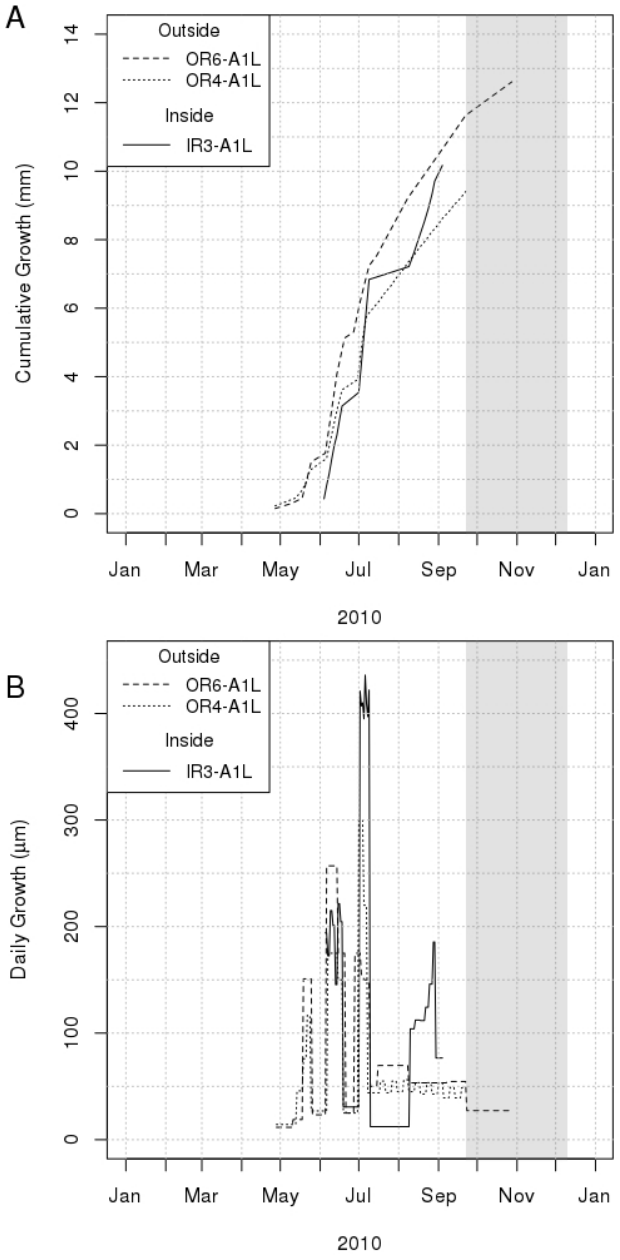

Figure 12: Growth curves for the three specimens that grew during 2010. (A) Cumulative growth curves. (B) Calculated daily growth rates. These data were obtained by dividing the distance between successive samples by the number of days between their assigned dates. The shaded region is the transplant interval.

ries is −7.30‰ and marks a ∼0.3‰ decline from the −7‰ plateau described above (Figure 5G). We assume this coincides with a similar drop in predicted $\delta^{18}O_{carb}$ values on July 8 (Figure 10). Sample 77 has a value of −5.17‰ and has the closest value to the last sample from OR4-A1L, which marks September 22. As above, we assume constant growth and assign samples dates every third day (Table 2).

The final OR6-A1L sample has a $\delta^{18}O_{carb}$ value of −3.91‰ (Table 2). The last day this value occurs in the oxygen isotope envelope is October 28, suggesting OR6-A1L stopped growing in late October approximately six weeks prior to collection. The intervening samples were linearly interpolated between September 22 and October 28 and assigned every sixth date (Table 2).

4.2.3. Inside Specimen: IR3-A1L

The inside specimen shows some of the same characteristics as the outside shells. Like OR4-A1L and OR6-A1L, the first samples (1 and 2; see Table 2) lie between −6 and −5‰ and precede a ∼2‰ drop in $\delta^{18}O_{carb}$ values (Figure 6). In turn, this drop predates a prominent growth line (Figure 6). These observations suggest samples 1 and 2 represent 2009 shell growth (Figure 11).

The remaining samples were deposited during 2010. The first 2010 sample (−6.59‰; Table 2) falls within the oxygen isotope envelope on June 4, 2010 (Figure 11). The following seven samples fit in the envelope between June 6 and June 18. The next nine samples (11-19) define a concave-down cycle and were assigned consecutive dates from July 1 through July 9 (Table 2). Following a one month gap in growth, samples 20-24 fit the envelope between August 9 and 24. Samples 25 and 26 lie just above the envelope on August 27 and 29 (0.17‰ and 0.09‰, respectively). That said, they closely track the overall trend in predicted $\delta^{18}O_{carb}$ values. The final value fits in the envelope on September 9 (Figure 11), suggesting 2010 growth ceased approximately two weeks before the mussel was collected on September 22.

IR3-A1L experienced two episodes with little to no growth in 2010, the first in late June and another spanning early July to early August. As with the outside specimens, these growth cessations coincide with intervals of rapidly increasing temperatures, suggesting intra-annual growth rates in *L. cardium* are sensitive to episodes of rapidly increasing water temperatures.

4.3. Patterns of Growth in L. cardium

Calibration of measured $\delta^{18}O_{carb}$ samples with the predicted oxygen isotope envelope establishes the timing of shell deposition. Plotting cumulative sample distances against sample dates generates growth curves for the three specimens that grew in 2010 (Figure 12). Together, with the oxygen isotope envelopes, these curves provide insight into the annual growth patterns of *L. cardium*.

4.3.1. Intra-Annual Growth

The two outside specimens (OR4-A1L and OR6-A1L) show similar patterns of growth (Figure 12A). After the initiation of shell deposition in late April, growth rates remained relatively low through the first half of May, increased briefly, then declined by latest May. The first half of June witnessed fast growth, and after another brief episode of slower growth, rates of shell precipitation increased again in early July. The remainder of the year saw relatively constant growth rates from both mussels.

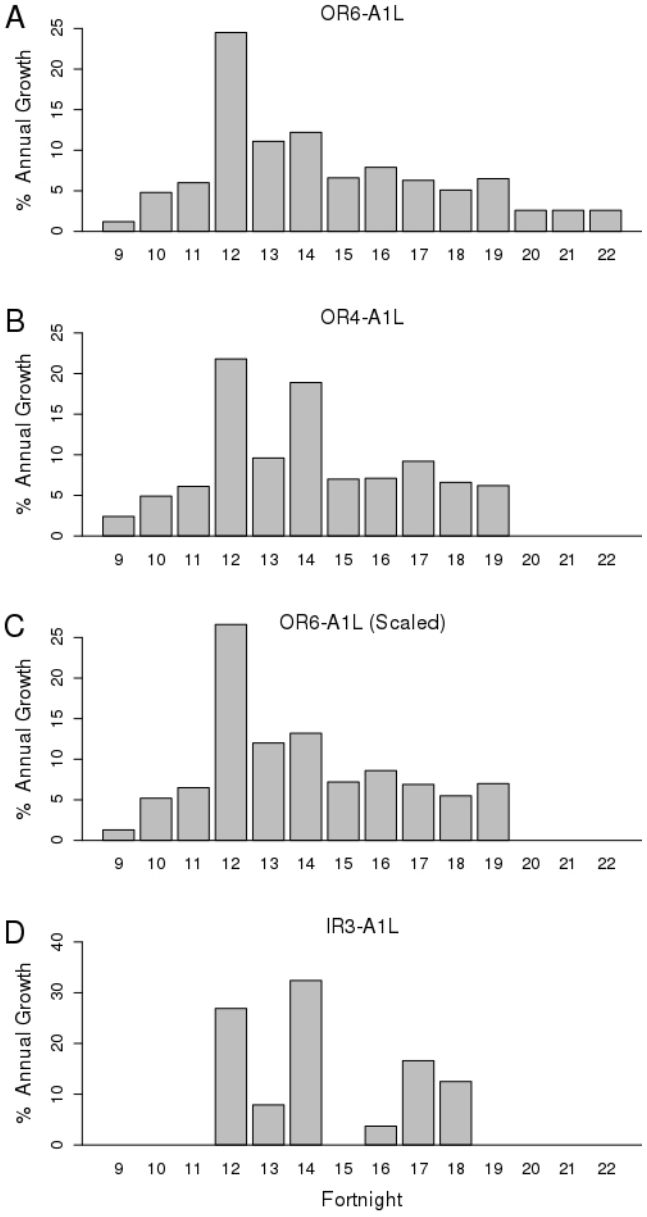

Figure 13: Biweekly percent annual growth for 2010. Fortnightly bins were employed because they capture high-frequency growth rate variation, highlight similarities and differences between specimens, and may facilitate comparison with marine bivalves whose growth commonly reflects tidal rhythms. A,B) Outside specimens, OR6-A1L and OR4-A1L. C) Growth of OR6-A1L assuming collection on September 22. D) Inside specimen, IR3-A1L.

Table 3: Biweekly percent growth for the three specimens that grew in 2010. Fortnight number reflects successive 14-day intervals in 2010 (i.e., Jan. 1–14, Jan. 15–28, Jan. 29–Feb. 11, etc.). Parenthetic values show biweekly percent growth for OR6-A1L assuming collection on September 22. See text for discussion.

Fortnight	Dates	OR6-A1L*	OR4-A1L	IR3-A1L
9	4/23–5/6	1.2 (1.3)	2.4	—
10	5/7–5/20	4.8 (5.2)	4.9	—
11	5/21–6/3	6.0 (6.5)	6.1	—
12	6/4–6/17	24.5 (26.6)	21.8	26.9
13	6/18–7/1	11.1 (12.0)	9.6	7.9
14	7/2–7/15	12.2 (13.2)	18.9	32.4
15	7/16–7/29	6.6 (7.2)	7.0	—
16	7/30–8/12	7.9 (8.6)	7.1	3.7
17	8/13–8/26	6.3 (6.9)	9.2	16.6
18	8/27–9/9	5.1 (5.5)	6.6	12.5
19	9/10–9/23	6.2 (7.0)	6.2	—
20	9/24–10/7	2.6 (—)	—	—
21	10/8–10/21	2.6 (—)	—	—
22	10/22–11/4	2.6 (—)	—	—

On September, 22 OR4-A1L was collected and OR6-A1L was transplanted inside. Following transplantation, the growth rates of OR6-A1L decreased slightly. Shell deposition in OR6-A1L ceased in late October.

The inside specimen shows a somewhat different pattern. Shell deposition in 2010 began more than a month later in early June and its initial growth rates were much greater than in the outside specimens. Following a significant growth rate decline in the second half of June, the fastest growth of the year occurred in early July (Figure 12A). Little or no shell was deposited between July 9 and August 9 (Table 2). Growth resumed in early August, continued through the month, and finally ceased in early September.

Figure 12B shows calculated *daily* growth rates for these mussels. These data were obtained by dividing the distance separating successive samples by the number of days between their assigned dates. The outside specimens display similar patterns of growth rate variation. Both mussels experienced pulses of rapid shell deposition in May, June, and July. OR6-A1L grew faster in than OR4-A1L in May and June, while the reverse was true in July. Peak growth rates during these three episodes were between 100 and 300 μm/day. Maximum daily growth rates for OR4-A1L and OR6-A1L were 300 μm/day and 257 μm/day, respectively. From mid-July to late September both grew at $\sim$50 μm/day. Following transplantation, growth in OR6-A1L slowed to approximately 25 μm/day. Initial growth rates of the inside specimen (June) were relatively high ($\sim$200 μm/day). In early July, IR3-A1L experienced the fastest growth of the year (436 μm/day). In each case, these episodes of rapid growth and coincide with relatively fast growth in the outside specimens (Figure 12B). Over the next month little, if any, shell was deposited. In early August, however, growth rates rebounded to between 100 and 150 μm/day. In latest August, growth rates declined before ceasing altogether in early September. Because of uncertainty in our date assignments (see Section 4.2.2), these daily grow rates are approximate.

Despite minor uncertainties, however, these daily growth rates are relatively high for freshwater mussels (see Haag, 2012), although not unprecedented (e.g., Kaandorp et al., 2003; Kelemen et al., 2017). Previous work has shown that rapid skeletal precipitation can lead to disequilibrium oxygen isotope fractionation (McConnaughey, 1989). Dettman et al. (1999), documented equilibrium oxygen iso-

tope fractionation in *L. cardium*. Furthermore, Goewert et al. (2007), working with *L. cardium* specimens that had growth rates comparable to those in this study, showed that $\delta^{18}O_{carb}$ samples agreed with calculated values. Accordingly, despite relatively rapid growth, we are confident that observed $\delta^{18}O_{carb}$ values accurately reflect environmental variation at the MRC.

To compare growth patterns we also calculated percent annual growth for successive biweekly bins (Table 3; Figure 13). Fortnightly bins were employed because they both capture high-frequency growth rate variation and highlight similarities and differences between specimens. This approach may also facilitate future comparison with marine bivalves whose growth often reflects tidal rhythms (e.g., Dettman et al., 2004). In both outside mussels (Figure 13A and 13B), growth rates progressively increased in fortnights 9–11, peaked in fortnights 12–14, and then declined through the remainder of the growing season. The fastest growth occurred in fortnight 12, followed by fortnights 14 and 13. This six week window accounts for ∼50% of all 2010 shell deposition in both specimens (Table 3). To further compare the growth of the outside specimens, fortnightly percents were recalculated assuming OR6-A1L was collected on September 22 (Table 3, parenthetic values; Figure 13C). These values are highly correlated with those from OR4-A1L (Spearman rank correlation: 0.909; p-value $\ll 0.001$). This high correlation is consistent with previous work showing that bivalves living at the same time and in the sample place have similar patterns of growth (Goodwin et al., 2004). Finally, approximately 7.8% of OR6-A1L shell growth occurred after it was transplanted. This suggests that the final sample distance from OR4-A1L would have been ∼10.2 mm if it had been transplanted inside with OR6-A1L.

In contrast, the growth of IR3-A1L is very different. Unlike outside specimens, which grew for more than six months, the inside specimen's growing season lasted only three months (Table 2; Figure 12). Shell deposition in 2010 was divided into two phases: fortnights 12–14 (early June through mid-June) and 16–18 (August through mid-September). Its initial growth was relatively fast, with the highest rates of shell deposition occurred in earliest July, followed by a month-long cessation (Table 2). Growth then resumed in August and continued through earliest September, when 2010 shell deposition ceased. The fastest growth of the year occurred in fortnight 14, when more than one-third of all 2010 shell deposition took place (Table 3). Finally, unlike OR6-A1L whose growth progressively slowed prior to shutting down, shell deposition on IR3-A1L halted abruptly in early September. Of course, it is possible that additional growth could have occurred if the specimen was collected later in the year.

The cumulative growth curves and biweekly percent growth data highlight the different growth patterns of outside and inside specimens. OR6-A1L grew 12.6 mm in 2010 (Table 2). OR4-A1L deposited 9.4 mm by September 22 and likely would have deposited ∼10.2 mm of shell if it was transplanted inside. IR3-A1L deposited more than 10.1 mm in 2010 (Table 2). Given that IR3-A1L deposited shell on only 93 days in 2010, it must have grown faster than the outside shells. Its average daily growth rate was approximately 109 μm/day, whereas OR4-A1L and OR6-A1L deposited 63 and 68 μm/day, respectively. Despite its abbreviated growing season, IR3-A1L added nearly as much shell material as the outside specimens.

The different intra-annual growth patterns exhibited by the outside and inside mussels may simply reflect individual variation. That said, the outside specimens show broadly similar patterns to each other (see Figure 12). The same, however, cannot be said for the inside specimen, because we only examined a single mussel. Analysis of additional specimens grown inside the MRC will be needed to confirm this difference.

To further investigate these growth patterns, we compared *seasonal* valve height measurements of the cohort from which the mussels used in the study were taken (Figure 9). At the time of the transplantation, the heights of the two populations were statistically indistinguishable (Student's t test: -1.1056; p-value $= 0.27$). However, after one growing season the outside specimens were significantly larger (Student's t test: -33.8861; p-value $\ll 0.001$). The outside shell heights had increased an average of 34.6 mm, while the inside specimens only added 6.2 mm—a difference of ∼2.8 cm. Over the 2008–2009 winter the shell heights in both groups remained essentially unchanged, which is consistent with the observation that *L. cardium* does not deposit shell during cold winter months (Dettman et al., 1999). After the 2009 growing season, however, the outside mussels added 17.4 mm and the inside mussels added 16.4 mm—a difference of 1 mm. These data suggest that the inside specimens grew significantly slower in the year following transplantation, but thereafter grew at nearly the same annual rate as those left outside.

Previous work has highlighted growth rate plasticity in transplanted unionoids. Kesler et al. (2007) illustrated that transplantation of mussels to a food limited environment negatively impacted shell growth in *Elliptio complanata*. Jokela and Mutikainen (1995) showed that shell growth rates and somatic mass decreased when *Anodonta piscinalis* was placed in resource limited settings. Roznere et al. (2014) documented physiological changes resembling starvation in the year following transplantation. Furthermore, Jokela (1996) showed that decreased somatic growth was linked to transplantation early in the growth season. Therefore, transplantation in April compounded by low Chl *a* concentrations (Figure 7), may have been responsible for the relatively slow growth of the inside specimens in 2008. Interestingly, annual growth rates of the inside specimens rebounded in 2009 (Figure 9), and were comparable to the outside specimens again in 2010 (Table 2). Some unionoids have shown tradeoffs between growth and reproductive effort in resource limited environments (e.g., Jokela, 1996). While we did not collect data on reproductive effort, it is possible that renewed

rapid growth in 2009 and 2010 was offset by reduced fecundity. Regardless of any putative compensatory mechanisms, however, renewed rapid growth of the inside specimens was accomplished with a completely different intra-annual pattern—at least in a single specimen. This observation suggests caution should be exercised when extrapolating intra-annual growth patterns from laboratory settings to natural populations.

4.3.2. Utility of the Oxygen Isotope Envelope

Calibrating observed $\delta^{18}O_{carb}$ values with the oxygen isotope envelope has two principal advantages over using predicted curves based solely on average daily temperatures. First, because the oxygen isotope envelope is defined using daily maximum and minimum temperatures, it provides a more complete picture of the range of possible $\delta^{18}O_{carb}$ values.

The second advantage of using the oxygen isotope envelope is related to the observation that bivalve growth rates may be biased toward optimal growth temperatures (Goodwin et al., 2001). This phenomenon is illustrated in Figure 10. Recall that samples 28–44 from OR4-A1L were assigned dates between July 12 and September 22 (see Section 4.2.2). Similarly, samples 52–76 from OR6-A1L were assigned dates in the same interval (Table 2). From mid-July through mid-August the $\delta^{18}O_{carb}$ values from both both specimens hug the positive edge of the envelope (Figure 10). Because of the inverse relationship between temperature and carbonate $\delta^{18}O$ values, the positive edge of the envelope corresponds with the coolest temperatures of the day, suggesting preferential growth in the cool early morning hours. In the second half of August $\delta^{18}O_{carb}$ values shift to the negative side of the envelope, where they remain until September 22. This transition suggests that, as temperatures fell in the late summer and early fall (see Figure 3A), these specimens grew fastest during the warm afternoon hours.

A corollary of this phenomenon is that the transition from one edge of the envelope to the other may mark the mussel's optimal growth temperatures. Between July 12 and August 20, when $\delta^{18}O_{carb}$ values track the positive edge of the envelope, average daily temperatures range between 30.4 and 27.3 °C. Following the shift to the negative side of the envelope, average temperatures fell to between 27.9 and 19.8 °C. These data suggest optimal growth temperatures near 27 to 28 °C. Furthermore, average temperatures during the transition (August 20–23) were between 27.1 to 29.6 °C. Additional support for this conclusion stems from the observation that, in both specimens, the fastest growth of the year occurred in latest June and earliest July (see Figure 12 and Section 4.2.2), when average temperatures were between 26 °C and 29 °C (see Figure 3). Taken together, these observations suggest that optimal growth temperatures in *L. cardium* are between 26 °C and 29 °C. They also highlight the utility of the oxygen isotope envelope as a powerful new tool for identifying optimal growth temperatures in bivalve mollusks.

Finally, that bivalves may bias daily growth toward their optimal growth temperatures has important implications for paleotemperature reconstruction. Given that these animals may be growing faster in the coolest morning hours during the hot summer, suggests that subsequent reconstructed paleotemperatures may be lower than actual average daily temperatures. The reverse may be true in the winter months. Thus, reconstructions of past seasonality may not capture that full range of temperature variability, even in species that grow throughout the year. Furthermore, it follows that the magnitude of this potential bias will depend on where optimal growth temperatures fall in the seasonal range of temperature. If optimal growth temperatures fall in the middle of the seasonal temperature range, the bias will be symmetrical. However, coincidence of optimal growth temperature with annual maximums, for example, may lead to significant overestimation of minimum temperature. Finally, the magnitude of this bias will depend on how sensitive bivalves are to deviations from their optimal growth temperatures. While this bias is not insurmountable, we do believe it should be considered in future analyses.

5. Conclusions

Oxygen isotope samples from five specimens of *Lampsilis cardium* collected in central Ohio were calibrated with a predicted oxygen isotope envelope calculated using high-resolution environmental records collected at the same site. From this analysis the following conclusions were drawn:

1. The close agreement between the observed and predicted $\delta^{18}O_{carb}$ profiles suggests that the specimens used in this study precipitated oxygen isotopes in equilibrium with the water in which they grew. This conclusion agrees with previous studies focused on *L. cardium*.
2. Calibration of the observed $\delta^{18}O_{carb}$ profiles from the outside specimens with predicted $\delta^{18}O_{carb}$ values indicates that the mussels collected in April contain little carbonate deposited during 2010. Mussels collected later in the year, however, have shell deposited in late April, suggesting the growing season began in mid- to late April. The specimen collected in September was actively depositing shell material when it was harvested, while shell growth in the other mussel halted in late October, nearly six weeks before it was collected. Taken together, these observations suggest the growing season extended from late April through late October.
3. The inside specimen had a much shorter growing season, with shell deposition taking place between early July and early September. The inside growth season is approximately half as long as outside.
4. Calculated daily growth rates were high early in the growing season and were somewhat episodic throughout the year. In all specimens, periodic growth cessations coincide with intervals of rapid increases in

water temperature, suggesting intra-annual growth rates in *L. cardium* are sensitive to episodes of rapidly increasing water temperatures.

5. Maximum daily growth rates for the outside and inside specimens were 300 and 436 μm/day, respectively.
6. Analysis of annual growth rates from the entire cohort suggests the inside specimens grew slower than the specimens left outside following initial relocation. In subsequent years, the two populations grew at similar rates. Our results suggest that, despite the fact that both populations have similar annual growth rates, they have different intra-annual growth patterns. Thus, caution should be exercised when extrapolating intra-annaul growth patterns from cultured specimens to natural populations.
7. Calibration of observed $\delta^{18}O_{carb}$ profiles with the oxygen isotope envelope, together with calculated daily growth rates, suggest optimal growth temperatures in *L. cardium* are between 26 °C and 29 °C.
8. The oxygen isotope envelope has several advantages over using predicted curves based on average daily temperatures, including: 1) providing the complete range of possible $\delta^{18}O_{carb}$ values; and, 2) the potential to identify optimal growth temperatures from calibrated isotope profiles.

6. Acknowledgements

Logistical support for this study was provided by the Columbus Zoo & Aquarium Freshwater Mussel Conservation & Research Center. Thanks also to Trisha Gibson, C. Brooke Kelly, and Jennifer Cecil for collecting geochemical samples. Special thanks to Jessica Rettig for help with chlorophyll fluorescence measurements. DHG thanks Tom Schultz for pointing in the right direction at the very beginning of the project. This manuscript benefitted from the thoughtful comments and constructive criticisms from Michael E. Böttcher and two anonymous reviewers. Funding for this work was provided by Denison University, Union College, a Keck Geology Consortium grant to DPG and DHG, and a Research Corporation for Science Advancement, Single-Investigator Cottrell College Science Award to DPG (#20169).

7. References

Black, B.A., Dunham, J.B., Blundon, B.W., Raggon, M.F., Zima, D., 2010. Spatial variability in growth-increment chronologies of long-lived freshwater mussels: Implications for climate impacts and reconstructions. Ecoscience 17, 240–250. doi:10.2980/17-3-3353.

Chamberlain, T.K., 1931. Annual growth of fresh-water mussels. Bulletin of the United States Bureau of Fisheries 46, 713–739.

Chauvaud, L., Lorrain, A., Dunbar, R.B., Paulet, Y.M., Thouzeau, G., Jean, F., Guarini, J.M., Mucciarone, D., 2005. Shell of the great scallop *Pecten maximus* as a high-frequency archive of paleoenvironmental changes. Geochemistry Geophysics Geosystems 6. doi:10.1029/2004GC000890.

Dansgaard, W., 1964. Stable isotopes in precipitation. Tellus 16, 436–468.

Dettman, D.L., Flessa, K.W., Roopnarine, P.D., Schöne, B.R., Goodwin, D.H., 2004. The use of oxygen isotope variation in shells of estuarine mollusks as a quantitative record of seasonal and annual colorado river discharge. Geochimica et Cosmochimica Acta 68, 1253–1263. doi:10.1016/j.gca.2003.09.008.

Dettman, D.L., Lohmann, K.C., 1995. Microsampling carbonates for stable isotope and minor element analysis: Physical separation of samples on a 20 micrometer scale. Journal of Sedimentary Research 65, 566–569.

Dettman, D.L., Lohmann, K.C., 2000. Oxygen isotope evidence for high-altitude snow in the laramide rocky mountains of north america during the late cretaceous and paleogene. Geology 28, 243–246.

Dettman, D.L., Reische, A.K., Lohmann, K.C., 1999. Controls on the stable isotope composition of seasonal growth bands in aragonitic fresh-water bivalves (unionidae). Geochimica et Cosmochimica Acta 63, 1049–1057.

Dunca, E., Mutvei, H., 2001. Comparison of microgrowth pattern in margaritifera margaritifera shells from south and north sweden. American Malacological Bulletin , 239–250.

Dycus, J.C., Wisniewski, J.M., Peterson, J.T., 2015. The effects of flow and stream characteristics on the variation in freshwater mussel growth in a southeast us river basin. Freshwater Biology 60, 395–409. doi:10.1111/fwb.12504.

Elliot, M., deMenocal, P.B., Linsley, B.K., Howe, S.S., 2003. Environmental controls on the stable isotopic composition of *Mercenaria mercenaria*: Potential application to paleoenvironmental studies. Geochemistry Geophysics Geosystems 4, 1–16. doi:10.1029/2002GC000425.

Epstein, S., Buchsbaum, R., Lowenstam, H., Urey, H.C., 1951. Carbonate-Water Isotopic Temperature Scale. Geological Society of America Bulletin 62, 417–426.

Ford, H.L., Schellenberg, S.A., Becker, B.J., Deutschman, D.L., Dyck, K.A., Koch, P.L., 2010. Evaluating the skeletal chemistry of mytilus californianus as a temperature proxy: Effects of microenvironment and ontogeny. Paleoceanography 25. doi:10.1029/2008PA001677.

Fritts, A.K., Fritts, M.W., Haag, W.R., DeBoer, J.A., Casper, A.F., 2016. Freshwater mussel shells (unionidae) chronicle changes in a north american river over the past 1000 years. Science of the Total Environment 575, 199–206. doi:10.1016/j.scitotenv.2016.09.225.

Fry, B., Allen, Y.C., 2003. Stable isotopes in zebra mussels as bioindicators of river–watershed linkages. River Research and Applications 19, 683–696. doi:10.1002/rra.715.

Gat, J.R., 1996. Oxygen and hydrogen isotopes in the hydrologic cycle. Annual Reviews of Earth and Planetary Science 24, 225–262.

Gat, J.R., Bowser, C.J., Kendall, C., 1994. The contribution of evaporation from the great lakes to the continental atmosphere: estimate based on stable isotope data. Geophysical Research Letters 21, 557–560.

Gillikin, D.P., Ridder, F.D., Ulens, H., Elskens, M., Keppens, E., Baeyens, W., Dehairs, F., 2005. Assessing the reproducibility and reliability of estuarine bivalve shells (*Saxidomus giganteus*) for sea surface temperature reconstruction: Implications for paleoclimate studies. Palaeogeography, Palaeoclimatology, Palaeoecology 228, 70–85. doi:10.1016/j.palaeo.2005.03.047.

Goewert, A., Surge, D., Carpenter, S.J., Downing, J., 2007. Oxygen and carbon isotope ratios of *Lampsilis cardium* (unionidae) from two streams in agricultural watersheds of iowa, usa. Palaeogeography, Palaeoclimatology, Palaeoecology 252, 637–648. doi:10.1016/j.palaeo.2007.06.002.

Gonfiantini, R., Stichler, W., Rozanski, K., 1995. Standards and intercomparison materials distributed by the international atomic energy agency for stable isotope measurements, in: Reference and Intercomparison Materials for Stable Isotopes of Light Elements, International Atomic Energy Agency, Vienna. pp. 13–29.

Goodwin, D., Flessa, K., Téllez-Duarte, M., Dettman, D., Schöne, B., Avila-Serrano, G., 2004. Detecting time-averaging and spatial

mixing using oxygen isotope variation: a case study. Palaeogeography Palaeoclimatology Palaeoecology 205, 1–21.

Goodwin, D.H., Cohen, A.N., Roopnarine, P.D., 2010. Forensics on the half shell: a sclerochronological investigation of a modern biological invasion in san francisco bay, united states. PALAIOS 25, 742–753. doi:10.2110/palo.2010.p10-015r.

Goodwin, D.H., Flessa, K.W., Schöne, B.R., Dettman, D.L., 2001. Cross-calibration of daily growth increments, stable isotope variation, and temperature in the gulf of california bivalve mollusk *Chione cortezi*: Implications for paleoenvironmental analysis. PALAIOS 16, 387–398.

Goodwin, D.H., Paul, P., Wissink, C.L., 2009. MoGroFunGen: A numerical model for reconstructing intra-annual growth rates of bivalve molluscs. Palaeogeography Palaeoclimatology Palaeoecology 276, 47–55.

Goodwin, D.H., Schöne, B.R., Dettman, D.L., 2003. Resolution and fidelity of oxygen isotopes as paleotemperature proxies in bivalve mollusk shells: Models and observations. PALAIOS 18, 110–125. doi:10.1669/0883-1351(2003)18<110:RAFOOI>2.0.CO;2.

Griffis, T.J., Wood, J.D., Baker, J.M., Lee, X., Xiao, K., Chen, Z., Welp, L.R., Schultz, N.M., Gorski, G., Chen, M., Nieber, J., 2016. Investigating the source, transport, and isotope composition of water vapor in the planetary boundary layer. Atmospheric Chemistry and Physics 16, 5139–5157. doi:10.5194/acp-16-5139-2016.

Grossman, E.L., Ku, T.L., 1986. Oxygen and carbon isotope fractionation in biogenic aragonite: temperature effects. Chemical Geology: Isotope Geoscience section 59, 59–74.

Haag, W.R., 2009. Extreme longevity in freshwater musses revisited: Sourses of bias in age estimates derived from mark-recapture experiments. Freshwater Biology 54, 1474–1486.

Haag, W.R., 2012. North American Freshwater Mussels: Natural History, Ecology, and Conservation. Cambridge University Press, New York.

Haag, W.R., Commens-Carson, A.M., 2008. Testing the assumption of annual shell ring deposition in freshwater mussels. Canadian Journal of Fisheries and Aquatic Sciences 65, 493–508. doi:10.1139/F07-182.

Haag, W.R., Rypel, A.L., 2011. Growth and longevity in freshwater mussels: evolutionary and conservation implications. Biological Reviews 86, 225–247. doi:10.1111/j.1469-185X.2010.00146.x.

Howard, A.D., 1921. Experiments in the culture of fresh-water mussels. Bulletin of the Unites States Bureau of Fisheries 38, 63–90.

Isely, F.B., 1913. Experimental study of the growth and migration of fresh-water mussels. Government Print Office, Washington D.C.

Jokela, J., 1996. Within-season reproductive and somatic energy allocation in a freshwater clam, *Anodonta piscinalis*. Oecologia 105, 167–174.

Jokela, J., Mutikainen, P., 1995. Phenotypic plasticity and priority rules for energy allocation in a freshwater clam: a field experiment. Oecologia 104, 122–132.

Kaandorp, R.J., Vonhof, H.B., Busto, C.D., Wesselingh, F.P., Ganssen, G.M., Marmól, A.E., Pittman, L.R., van Hinte, J.E., 2003. Seasonal stable isotope variations of the modern amazonian freshwater bivalve *Anodontites trapesialis*. Palaeogeography, Palaeoclimatology, Palaeoecology 194, 339–354. doi:10.1016/S0031-0182(03)00332-8.

Kelemen, Z., Gillikin, D.P., Graniero, L.E., Havel, H., Darchambeau, F., Borges, A.V., Yambele, A., Bassirou, A., Bouillon, S., 2017. Calibration of hydroclimate proxies in freshwater bivalve shells from central and west africa. Geochimica et Cosmochimica Acta 208, 41–62. doi:10.1016/j.gca.2017.03.025.

Kesler, D.H., Newton, T.J., Green, L., 2007. Long-term monitoring of growth in the eastern elliptio, *Elliptio complanata* (bivalvia: Unionidae), in rhode island: a transplant experiment. Journal of the North American Benthological Society 26, 123–133.

Killingley, J.S., Berger, W.H., 1979. Stable isotopes in a mollusk shell: Detection of upwelling events. Science 205, 186–188.

Kirby, M.X., Sonait, T.M., Spero, H.J., 1998. Stable isotope sclerochronology of pleistocene and recent oyster shells (*Crassostrea virginica*). PALAIOS 13, 560–569.

Klein, R.T., Lohmann, K.C., Thayer, C.W., 1996. Bivalve skeletons record sea-surface temperature and $\delta^{18}O$ via Mg/Ca and $^{18}O/^{16}O$ ratios. Geology 24, 415–418.

Kraemer, L.R., 1970. The mantle flap in three species of *Lampsilis* (pelecypoda: Unionidea). Malacologia 10, 225–282.

Lazareth, C.E., Guzman, N., Poitrasson, F., Candaudap, F., Ortlieb, L., 2007. Nyctemeral variations of magnesium intake in the calcitic layer of a chilean mollusk shell (*Concholepas concholepas*, gastropoda). Geochimica et Cosmochimica Acta 71, 5369–5383.

Lazareth, C.E., Lasne, G., Ortlieb, L., 2006. Growth anomalies in *Protothaca thaca* (mollusca, veneridae) shells as markers of enso conditions. Climate Research 30, 263–269.

McConnaughey, T., 1989. ^{13}c and ^{18}o isotopic disequilibrium in biological carbonates: I. patterns. Geochimica et Cosmochimica Acta 53, 151–162.

Negus, C., 1966. A quantitative study of the growth and production of unionid mussels in the River Thames at Reading. Journal of Animal Ecology 35, 513–532.

NWS, 2011. National weather service forecast office wilmington, oh. URL: http://www.weather.gov/iln/.

Poulain, C., Lorrain, A., Flye-Sainte-Marie, J., Amice, E., Morize, E., Paulet, Y.M., 2011. An environmentally induced tidal periodicity of microgrowth increment formation in subtidal populations of the clam *Ruditapes philippinarum*. Journal of Experimental Marine Biology and Ecology 397, 58–64.

Poulain, C., Lorrain, A., Mas, R., Gillikin, D., Dehairs, F., Robert, R., Paulet, Y.M., 2010. Experimental shift of diet and dic stable carbon isotopes: In uence on shell δ^{13}c values in the manila clam *Ruditapes philippinarum*. Chemical Geology 272, 75–82.

Rafinesque, C., 1820. Monographe des coquilles bivalves fluviatiles de la rivière ohio, contenant douze genres et soixante huit espèces. Annales Generales des Sciences Physique, Bruxelles 5, 287–322.

Ricciardi, A., Rasmussen, J.B., 1999. Extinction rates of north american freshwater fauna. Conservation Biology 13, 1220–1222.

Richardson, C., 2001. Molluscs as archives of environmental change. Oceanography and Marine Biology Annual Review 39, 103–164.

Roznere, I., Watters, G.T., Wolfe, B.A., Daly, M., 2014. Nontargeted metabolomics reveals biochemical pathways altered in response to captivity and food limitation in the freshwater mussel *Amblema plicata*. Comparative Biochemistry and Physiology, Part D 12, 53–60.

Rypel, A.L., Haag, W.R., Findlay, R.H., 2008. Validation of annual growth rings in freshwater mussel shells using cross dating. Canadian Journal of Fisheries and Aquatic Sciences 65, 2224–2232. doi:10.1139/F08-129.

Schöne, B.R., 2008. The curse of physiology—challenges and opportunities in the interpretation of geochemical data from mollusk shells. Geo-Marine Letters 28, 269–285. doi:10.1007/s00367-008-0114-6.

Schöne, B.R., Dunca, E., Fiebig, J., Pfeiffer, M., 2005. Mutvei's solution: An ideal agent for resolving microgrowth structures of biogenic carbonates. Palaeogeography, Palaeoclimatology, Palaeoecology 228, 149–166. doi:10.1016/j.palaeo.2005.03.054.

Schöne, B.R., Dunca, E., Mutvei, H., Norlund, U., 2004. A 217-year record of summer air temperature reconstructed from fresh water pearl mussels (*M. margarifitera*, sweden). Quaternary Science Reviews 23, 1803–1816.

Schöne, B.R., Tanabe, K., Dettman, D.L., Sato, S., 2003. Environmental controls on shell growth rates and $\delta^1$8o of the shallow-marine bivalve mollusk *Phacosoma japonicum* in japan. Marine Biology 142, 473–485.

Sharp, Z., 2006. Principles of Stable Isotope Geochemistry. 1^{st} edition ed., Prentice Hall, New York.

Thébault, J., Chauvaud, L., Clavier, J., Fichez, R., Morize, E., 2006. Evidence of a 2-day periodicity of striae formation in the tropical scallop *Comptopallium radula* using calcein marking. Marine Biology 149, 257–267.

Tynan, S., Dutton, A., Eggins, S., Opdyke, B., 2014. Oxygen isotope records of the australian flat oyster (*Ostrea angasi*) as a potential temperature archive. Marine Geology 357, 195–209. doi:10.1016/j.margeo.2014.07.009.

Urey, H.C., 1948. Oxygen Isotopes in Nature and in the Laboratory. Science (New York, N.Y.) 108, 489–496.

Urey, H.C., Lowenstam, H.A., Epstein, S., McKinney, C.R., 1951. Measurement of Paleotemperatures and Temperatures of the Upper Cretaceous of England, Denmark, and the Southeastern United States. Geological Society of America Bulletin 62, 399–416.

USGS, 2011. United states geological survey, national water information system. URL: http://waterdata.usgs.gov/nwis/.

Versteegh, E.A.A., Troelstra, S.R., Vonhof, H.B., Kroon, D., 2009. Oxygen isotope composition of bivalve seasonal growth increments and ambient water in the rivers rhine and meuse. PALAIOS 24, 497–504. doi:10.2110/palo.2008.p08-071r.

Versteegh, E.A.A., Vonhof, H.B., Troelstra, S.R., Kaandorp, R.J.G., Kroon, D., 2010. Seasonally resolved growth of freshwater bivalves determined by oxygen and carbon isotope shell chemistry. Geochemistry Geophysics Geosystems 11. doi:10.1029/2009GC002961.

Wanamaker, A D, J., Kreutz, K.J., Borns, H W, J., Introne, D.S., Feindel, S., Funder, S., Rawson, P.D., Barber, B.J., 2007. Experimental determination of salinity, temperature, growth, and metabolic effects on shell isotope chemistry of *Mytilus edulis* collected from maine and greenland. Paleoceanography 22, PA2217. doi:10.1029/2006PA001352.

Watters, G.T., Hoggarth, M.A., Stansbery, D.H., 2009. The Freshwater Mussles of Ohio. The Ohio State University Press, Columbus.

Welschmeyer, N.A., 1994. Fluorometric analysis of chlorophyll *a* in the presence of chlorophyll *b* and pheopigments. Limnology and Oceanography 39, 1985–1992.

Williams, J.D., Warren, M.L., Cummings, K.S., Harris, J.L., Neves, R.J., 1993. Conservation status of freshwater mussels of the united states and canada. Fisheries 18, 6–22.